Discovery of *N*-[(3*R*)-1-Azabicyclo[2.2.2]oct-3-yl]furo[2,3-*c*]pyridine-5-carboxamide, an Agonist of the α7 Nicotinic Acetylcholine Receptor, for the Potential Treatment of Cognitive Deficits in Schizophrenia: Synthesis and Structure−Activity Relationship

Donn G. Wishka, Daniel P. Walker, Karen M. Yates, Steven C. Reitz, Shaojuan Jia, Jason K. Myers, Kirk L. Olson, E. Jon Jacobsen, Mark L. Wolfe, Vincent E. Groppi, Alexander J. Hanchar, Bruce A. Thornburgh, Luz A. Cortes-Burgos, Erik H. F. Wong, Brian A. Staton, Thomas J. Raub, Nicole R. Higdon, Theron M. Wall, Raymond S. Hurst, Rodney R. Walters, William E. Hoffmann, Mihaly Hajos, Stanley Franklin, Galen Carey, Lisa H. Gold, Karen K. Cook, Steven B. Sands, Sabrina X. Zhao, John R. Soglia, Amit S. Kalgutkar, Stephen P. Arneric, and Bruce N. Rogers*

Pfizer Global Research & Development, Eastern Point Road, Groton, Connecticut 06340

Received March 1, 2006

N-[(3*R*)-1-Azabicyclo[2.2.2]oct-3-yl]furo[2,3-*c*]pyridine-5-carboxamide (**14**, PHA-543,613), a novel agonist of the α7 neuronal nicotinic acetylcholine receptor (α7 nAChR), has been identified as a potential treatment of cognitive deficits in schizophrenia. Compound **14** is a potent and selective α7 nAChR agonist with an excellent in vitro profile. The compound is characterized by rapid brain penetration and high oral bioavailability in rat and demonstrates in vivo efficacy in auditory sensory gating and, in an in vivo model to assess cognitive performance, novel object recognition.

Introduction

Schizophrenia is a chronic and highly debilitating disease afflicting over three million people in the U.S.[1] This complex disorder is characterized by a constellation of symptoms, including positive (hallucinations, delusions), negative (apathy, withdrawal), and cognitive. Significant advances have been made in therapies for the treatment of the positive and negative symptoms of schizophrenia, but the vast majority of schizophrenic patients (85%) are also reported to suffer from cognitive deficits that remain largely untreated.[2]

It is believed that neuronal nicotinic acetylcholine receptors (nAChRs) are involved in a variety of attention and cognitive processes.[3] These calcium-permeable, ligand gated ion channels modulate synaptic transmission in key regions of the central nervous system (CNS) involved in learning and memory, including the hippocampus, thalamus, and cerebral cortex.[4] Among the nAChRs, physiological,[5] pharmacological,[6] and human genetic[7] data suggest a link between the α7 nAChR and cognitive deficits in schizophrenia.

One of the measurable neurophysiological abnormalities in schizophrenic patients, P50 auditory gating deficit, indicates an impaired information processing and a diminished ability to "filter" unimportant or repetitive sensory information. On the basis of the clinical observation that these deficits are acutely normalized by nicotine,[8] it has been suggested that the high prevalence of heavy smoking among patients with schizophrenia (>80%) may be a form of self-medication.[9] Limited human studies suggest that nicotine's mechanism of action in cognition is via the α7 nAChR.[10] Restoration of P50 gating deficits in rodent models has been demonstrated with the α7 nAChR partial agonist **1 (**GTS-21)[11] and with the selective α7 nAChR agonists such as **2 (**PNU-282,987).[12] Additionally, human studies with **1** suggest the potential for an enhancement of cognitive function.[13] Improvements in sensory processing are thought to correlate with enhanced cognitive performance in animal models and in patients with schizophrenia,[14] suggesting the potential for a beneficial role of a selective α7 nAChR agonist in the treatment of impaired cognitive function through the modulation of sensory processing.

The structural (chemical) diversity of nicotinic ligands has expanded greatly over the past decade, with a focus on identification of selective agents.[15] Early compounds, which assisted greatly in the evolution of the α7 nAChR field, include ligands such as the anabasine analogue **1**[16] and the spirooxazolidinone **3 (**AR-R17779).[17] Many of the recent ligands disclosed in the literature come from the azabicyclic diamine scaffold and include such structures as quinuclidine carbamates,[18] amides,[19] ethers,[20] and 1,4-diazabicyclo[3.2.2]nonanes such as **4** (SSR180711A).[21]

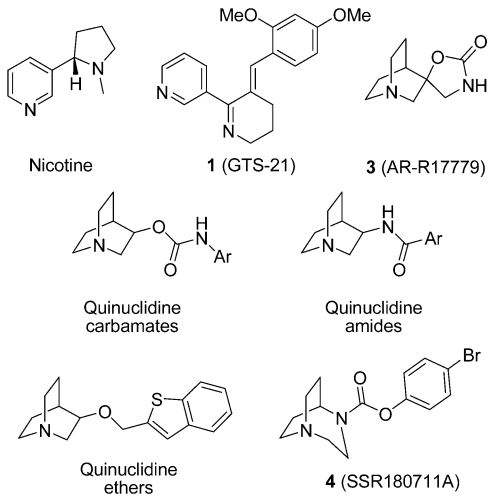

Early in our α7 nAChR program, utilizing high-throughput screening and parallel synthetic chemistry, the quinuclidine amide **2** was identified as a potent and selective agonist of the α7 nAChR.[19] This compound was later found, however, to possesses significant hERG (human ether-a-go-go) potassium channel activity and thus did not meet our criteria for further development. Additional work on this template demonstrated that fused 6,5-heterocyclic analogues, such as indole **5**, provided

* To whom correspondence should be addressed: Phone: 860-686-0545. Fax: 860-686-5403. E-mail: bruce.n.rogers@pfizer.com.

10.1021/jm0602413 CCC: $33.50
Published on Web 06/10/2006

an avenue toward novel analogues with potential for improved safety profiles. We detail below the synthesis and biological profiles of a set of novel 6,5-fused analogues and the initial pharmacokinetic and efficacy profile of this series of 6,5-fused heteroaromatic quinuclidine carboxamides.

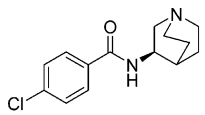

2 (PNU-282,987)

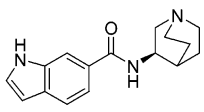

5

Chemistry

Our program objective was to identify an improved candidate with potent in vitro functional and binding activity at the α7 nAChR, low first-pass metabolism, and a favorable hERG profile. To expand the SAR around indole **5**, novel monosubstituted heteroarylcarboxamides of general structure **6** were targeted and prepared according to Scheme 1.[22] Treatment of (*R*)-3-aminoquinuclidine with a custom heteroarylcarboxylic acid, using *O*-(7-azabenzotriazole-1-yl)-*N*,*N*,*N*′,*N*′-tetramethyluronium hexafluorophosphate (HATU), diphenylphosphorylazide (DPPA), or phosphoric acid bis(2-oxooxazolidide) chloride (BOP-Cl), gave rise to the corresponding quinuclidine benzamides (**6**). In general, the HATU conditions afforded cleaner products in higher yields. The corresponding custom acid fragments were prepared via multistep synthesis.[22] Over 100 analogues of this type were prepared,[23] and this paper will focus on a subset of these compounds (Table 1).

Results and Discussion

Indole **7**, a regioisomer of **5**, shows a 5-fold decrease in α7 nAChR activity, as demonstrated by a primary α7-5HT$_3$ chimera FLIPR assay.[24] Saturation of the five-membered ring of indole **7** produced indoline **8**, which also shows a significant decrease in activity. As noted in our earlier communication,[19] the α7 receptor is sensitive to subtle changes made in the aromatic ring of this class of compounds. Thiophenes **9** and **10** both possess enhanced potency toward α7, and **10** also demonstrates reasonable stability in rat liver microsomes (RLM). Changing the indole nitrogen of **7** to oxygen afforded benzofuran **11**, which was the first compound in this series that not only possesses good activity in the α7-5HT$_3$ FLIPR assay and excellent α7 binding activity but also shows good stability in rat microsomes. Regioisomeric benzofuran **13** displayed potency and stability similar to the potency and stability of benzofuran **11**. Dihydrobenzofuran **12** possesses potency similar to that of benzofuran **11**; however, it is unstable in microsomes.

While the metabolic stability of benzofurans **11** and **13** in microsomes was encouraging, it is known that some benzofuran-containing compounds undergo metabolic activation on the furan ring, generating reactive metabolites.[25] The electron-rich nature of the furan ring presumably facilitates metabolic activation. It was hypothesized that the replacement of one of the carbon atoms in the six-membered aromatic ring with a nitrogen atom, generating a furopyridine, would attenuate the potential metabolic liability of the furan ring. Four different furopyridine analogues were prepared (**14**−**17**, Table 1). In general, it was found that the furopyridine analogues are less potent than the corresponding benzofuran compounds. The magnitude of potency loss clearly depends on the position of the nitrogen in the furopyridine ring. While furo[2,3-*c*]pyridine **14** demonstrates a modest decrease in affinity compared to the corresponding benzofuran **11**, furo[2,3-*b*]pyridine **15** is inactive up to the highest dose tested (10 μM). A similar trend was observed for the 6-substituted furopyridines **16** and **17**. Hence, while the potency of furo[3,2-*c*]pyridine **16** is comparable to that of the corresponding benzofuran (**13**), furo[3,2-*b*]pyridine **17** shows a significant loss of potency. Both furopyridines **14** and **16** demonstrate reasonable RLM stability; however, only compound **14** met our potency criteria. Once the preferred position of the nitrogen had been established in the furopyridine series, the corresponding thienopyridines and a pyrrolopyridine were prepared (**18**−**20**). Although both thienopyridines possess good potency and affinity similar to their benzothiophene counterparts, neither analogue is stable in the microsomal stability assay. While pyrrolopyridine **20** did possess activity similar to that of

Scheme 1[a]

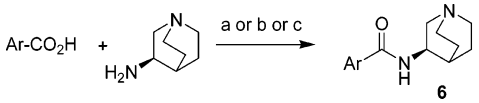

[a] Reagents and conditions: (a) *O*-(7-azabenzotriazole-1-yl)-*N*,*N*,*N*′,*N*′-tetramethyluronium hexafluorophosphate (HATU), *i*Pr$_2$NEt, DMF, 0 °C to room temperature; (b) diphenylphosphorylazide (DPPA), Et$_3$N, CH$_2$Cl$_2$, room temp; (c) phosphoric acid bis(2-oxooxazolidide) chloride (BOP-Cl), Et$_3$N, CH$_2$Cl$_2$, DMF.

Table 1. In Vitro α7 nAChR[a] Activity and Rat Liver Microsome Profile

Cpd#	Ar	α7-5HT$_3$[b] chimera EC$_{50}$ (nM) ± SEM	α7[c] K$_i$ (nM) ± SEM	in vitro[d] RLM (% remain)
2		128	24 ± 8	96
5		100	NT	14
7		550	NT	NT
8		600	83 ± 0.5	NT
9		55 ± 13	6.9 ± 0.3	6
10		48 ± 16	2.1 ± 0.1	29
11		47 ± 4	1.6 ± 0.3	77
12		77 ± 10	15 ± 2.0	9
13		86 ± 11	12.5 ± 0.5	69
14		65 ± 11	8.8 ± 1.3	55
15		>10,000	NT	NT
16		374 ± 120	50.0 ± 5.0	40
17		>10,000	NT	NT
18		100 ± 13	6.3 ± 1.0	7
19		81 ± 9	5.0 ± 2.5	7
20		1173 ± 37	NT	29

[a] Average of at least five experiments, except **5**, **7**, and **8**. [b] Compounds tested in a cell-based FLIPR assay using SH-EP1 cells expressing the α7 5HT$_3$ chimera. [c] Rat brain homogenate binding assay, [^{3}H]MLA, with average of two or more experiments. [d] In vitro metabolism in rat liver microsomes, expressed as percent remaining at 1 h.

Table 2. In Vitro Selectivity for Select Compounds

			nicotinic selectivity data			
compd	5-HT_3 binding $K_i \pm$ SEM (nM)	5-HT_3 functional[a,b] $K_i \pm$ SEM (nM)	$\alpha3\beta4$[a,c] IC_{50} (μM)	$\alpha1\beta1\gamma\delta$[a,d] IC_{50} (μM)	$\alpha4\beta2$[e] % inhibition	hERG % block @ 2, 20 μM[f]
2	1662	4540	>60	>60	14	11, 57
10	174 ± 46	188 ± 27	38	>100	NT	13, 65
11	663 ± 99	580 ± 46	>100	>100	5	2, 33
13	310 ± 8	962 ± 54	81	>100	NT	2, 29
14	511 ± 29	628 ± 83	>100	>100	13	NT, 29

[a] FLIPR cell-based functional assays.[22] [b] SH-EP1 expressing 5-HT_3 cells. [c] SH-SY5Y cells, $\alpha3\beta4$-containing. [d] TE671 cells, native $\alpha1\beta1\gamma\delta$. [e] Rat brain homogenate binding assay, [^{3}H]cytisine, % block, 1 μM. [f] In vitro effect on hERG current (IKr), HEK cells.

indole **7**, the modest potency did not support further evaluation of this compound.

On the basis of the data in Table 1, four compounds were selected for further profiling: benzothiophene **10**, benzofurans **11** and **13**, and furopyridine **14**. The four compounds were evaluated for functional selectivity against the 5-HT_3 receptor expressed in SH-EP1 cells, endogenous receptors of TE671 to evaluate the muscle-like nAChR ($\alpha1\beta1\gamma\delta$), and endogenous receptors of SH-SY5Y cells to evaluate the ganglion-like nAChRs ($\alpha3\beta4$) (Table 2). Each of the four compounds possesses antagonist activity at the 5-HT_3 receptor. That the greatest degree of cross-reactivity was observed with the 5-HT_3 serotonin receptor is not surprising given the high degree of homology between orthosteric sites in $\alpha7$ nAChRs and 5-HT_3 receptors. Each compound provided at least 25-fold binding selectivity and a functional preference for the $\alpha7$ nAChR. The relative risk associated with antagonism of the 5-HT_3 receptor was considered to be low, in contrast to concerns that would have arisen had the compounds been found to possess agonist activity at this receptor. In fact, recent clinical studies suggest that the potent and selective 5-HT_3 receptor antagonist ondansetron is well tolerated in patients with schizophrenia following 12 weeks of treatment and may provide a benefit for tardive dyskinesia and psychotic symptoms.[26] Compounds **10**, **11**, **13**, and **14** show no detectible agonist activity (>100 μM) and negligible antagonist activity at both muscle-like nAChRs (TE671 cells) and ganglion-like nAChRs (SH-SY5Y cells). Further, the compounds do not significantly displace tritiated cytisine from rat brain homogenates at 1 μM, suggesting a selectivity over the $\alpha4\beta2$ nAChR subtype.

As part of our discovery program for advancing lead compounds, in vitro cardiovascular safety was assessed (Table 2). Prolongation of the QT interval is believed to increase the risk of cardiac arrhythmia in humans and could potentially lead to ventricular fibrillation.[27a] Measuring the ability of a compound to block the hERG potassium channel is an important preclinical assay to assess the compound's proarrhythmic potential.[27b] Compounds **2**, **10**, **11**, **13**, and **14** were evaluated in a patch-clamp hERG K^+ channel assay at 2 and 20 μM.[28] Benzothiophene **10** inhibits hERG at levels similar to that of **2**. These levels of inhibition are considered high on the basis of the efficacious drug concentrations of **2**.[12,19] Benzofurans **11** and **13** and furopyridine **14** all show reduced hERG inhibition at 20 μM, which may be the result of replacing the sulfur atom with the less lipophilic oxygen atom.[29] To further evaluate the interactions with the hERG potassium channel, concentration response profiles were determined for **2** and **14**. In agreement with the screening data, **14** is less potent at inhibiting the hERG channel-mediated currents. While **14** produces insufficient blockade at the highest tested concentration of 20 μM to establish an IC_{50}, extrapolating the blockade produced at this concentration (29% for **14**) to the fitted curve for **2** suggests that the potency for blocking hERG is reduced by at least 10-fold (Figure 1).

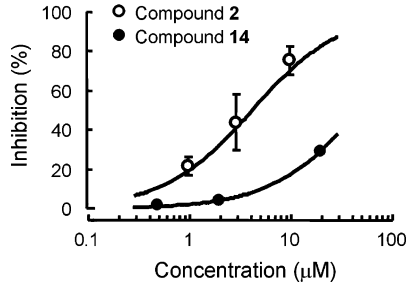

Figure 1. hERG potassium channel concentration response profiles of **2** and **14**.

While the metabolic stability of benzofurans **11** and **13** in liver microsomes was encouraging, the presence of the furan motif in these derivatives was of some concern given the propensity of this ring system to undergo P450-catalyzed bioactivation to electrophilic intermediates, which are capable of covalently reacting with cellular biomacromolecules including P450 enzymes and eliciting a toxicological response.[25] Consequently, the ability of benzofurans **11** and **13** and furopyridine **14** to undergo oxidative bioactivation in human liver microsomes (HLM) was examined in the reactive metabolite assay (RMA) (Table 3).[30] The RMA assesses a compound's ability to undergo metabolic activation in HLM by generating glutathione-captured metabolites.[25] Glutathione ethyl ester (GSH-EE) was used as the exogenous trapping agent in the microsomal incubations based on previous studies from our laboratories that revealed the improved sensitivity in sulfydryl conjugate detection with the ethyl ester derivative of GSH relative to the free carboxylic acid analogue.[25]

Compound **13** is positive in the RMA, which confirmed our concerns about the potential metabolic liability of benzofurans. LC/MS/MS analysis of NADPH-supplemented human liver microsomal incubations containing **13** and GSH-EE led to the detection of a single conjugate with a molecular ion (MH^+) at 604.[31] The molecular mass of this conjugate was consistent with the addition of one molecule of GSH-EE to the molecular mass of the parent compound **13**. The product ion spectrum obtained by collision-induced dissociation of the MH^+ at 604 produced diagnostic fragment ions at *m*/*z* 475 and 334.[31] The fragment ion at *m*/*z* 475 was consistent with the characteristic loss of the pyroglutamate moiety in GSH-EE and related analogues,[32] whereas the fragment ion at *m*/*z* 334 localized the site of bioactivation and subsequent sulfydryl conjugation on the benzofuran ring. In theory, metabolic activation of the benzofuran ring system (Scheme 2) can occur via P450-catalyzed epoxidation on the benzene ring (pathway a) or the furan ring (pathway b).[25] In each of these scenarios, addition of GSH-EE across the electrophilic epoxide intermediate followed by subsequent dehydration would result in the formation of the

Table 3. The in Vitro and in Vivo Pharmacokinetic Profiles for Select Compounds

			HLM[b]		RLM[c]		rat[d]		MBUA[e]
compd	RMA (HLM)[a]	CYP2D6 IC_{50} (nM)	CL hep ($mL \cdot min^{-1} \cdot kg^{-1}$)	$T_{1/2}$ (min)	CL hep ($mL \cdot min^{-1} \cdot kg^{-1}$)	$T_{1/2}$ (min)	CL ($mL \cdot min^{-1} \cdot kg^{-1}$)	F (%)	brain/plasma @ 5, 60 min
2	NT	>3000	<5.3	>120	<20.0	>120	30	74	0.8, 5.0
11	neg	3600	<5.3	>120	<20.1	>120	39	88	0.38, 1.24
13	pos	>10000	<5.3	>120	NT	NT	58	76	0.86, 2.96
14	neg	>10000	<5.3	>120	38.9	40	50	63	1.5, 1.5

[a] RMA: reactive metabolite assay with HLM. [b] HLM: human liver microsomes, in vitro compound lability. [c] RLM: rat liver microsomes, in vitro compound lability. [d] Clearance and oral bioavailability determined in constant infusion model. [e] MBUA: mouse brain uptake assay; brain/plasma = (concentration in brain)/(concentration in plasma).

Scheme 2. Proposed Bioactivation Pathways of Benzofuran Derivative **13**

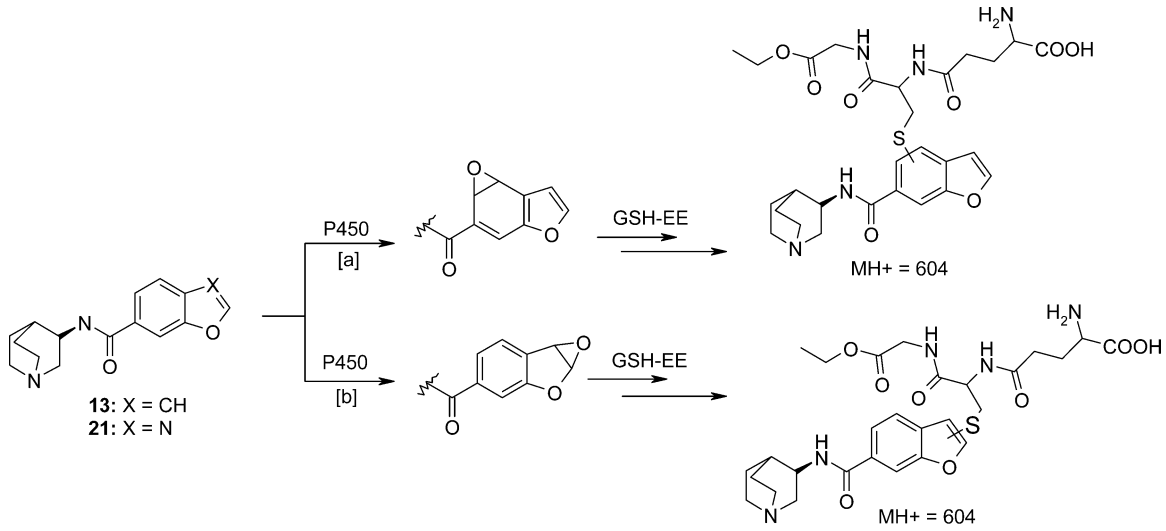

sulfydryl conjugate of **13** with an MH^+ at 604 amu. In an attempt to distinguish between the two potential bioactivation pathways, the corresponding benzoxazole derivative of **13**, compound **21** (see Scheme 2), was prepared and examined in the RMA assay. No sulfydryl conjugates of benzoxazole **21** were discernible in NADPH and GSH-EE fortified HLMs. Overall, the lack of detection of GSH-EE conjugate(s) of **21** in this analysis is consistent with the known biotransformation pathways of benzoxazoles, which do not involve a P450-mediated metabolic activation component in a manner similar to that noted with corresponding furans.[33] On the basis of these observations, it is proposed that the mechanism of P450-catalyzed bioactivation of benzofuran **13** that leads to the observed sulfydryl conjugate most likely proceeds via pathway b shown in Scheme 2. Because of the potential metabolic liability of benzofuran **13**, it was not considered for further evaluation. Interestingly, the 5-substituted benzofuran **11** and furopyridine **14** are clean in the RMA. Presumably, the position of the electron-withdrawing carboxamide influences the metabolic reactivity of the furan ring.

Further human and rat in vitro pharmacokinetic (PK) evaluation demonstrated moderate clearance and half-lives for compounds **2**, **11**, **13**, and **14** (Table 3). In vivo PK evaluation in a rat constant infusion model verified the in vitro PK data and predicted good oral bioavailability of >60% for each of the compounds and clearance consistent with the RLM data. Differentiation of the compounds came from CYP2D6 evaluation, where benzofuran **11** was found to inhibit this key P450 enzyme. Fortunately, furopyridine **14** is inactive up to the highest dose tested (10 μM). Finally, a mouse brain uptake assay (MBUA) was used to evaluate CNS penetration.[34] Compounds **2**, **11**, **13**, and **14** each have excellent brain penetration; however, with the exception of furopyridine **14** each demonstrates a modest accumulation in the CNS. Brain accumulation was not a desirable attribute, given the α7 receptor's known desensitization profile.[35] A separate PK study evaluating **14**, utilizing a 5 mg/kg dose in rat, is in close agreement with the infusion data above: 65% oral bioavailability, low clearance of 33.3 $mL \cdot min^{-1} \cdot kg^{-1}$, and volume of distribution of 1.8 $L \cdot kg^{-1}$. On the basis of the data presented, compound **14** clearly differentiates itself from **2**, **11**, and **13**, justifying further in vivo evaluation.[36]

The functional activity of **14** was confirmed with native α7 nAChRs of rat hippocampal neurons (Figure 2). When rapidly applied to neurons recorded in the whole-cell patch clamp configuration, **14** evokes desensitizing inward currents that are concentration-dependent and completely inhibited by the selective α7 nAChR antagonist methyllycaconitine (MLA, 10 nM). The response amplitude evoked upon application of **14** at 0.3, 3, and 30 μM was 34 $\pm$ 1%, 103 $\pm$ 7%, and 220 $\pm$ 22%, respectively, of the response evoked by 100 μM (−)-nicotine applied to the same cell. These results suggest that **14** is modestly more active than **2** at native α7 nAChRs,[12] which is consistent with the increased potency reported here in both the binding assay and the FLIPR assay using the α7 $5HT_3$ chimera.

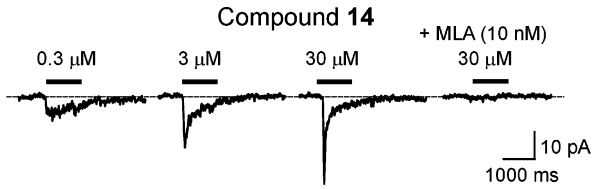

Figure 2. Compound **14** evokes α7 nAChR-mediated currents from rat hippocampal neurons (n = 3).

Compound **14** was also tested in a validated rodent model of impaired sensory gating.[11,12] Administration of *d*-amphetamine (1 mg/kg, iv) significantly disrupts hippocampal CA3 region

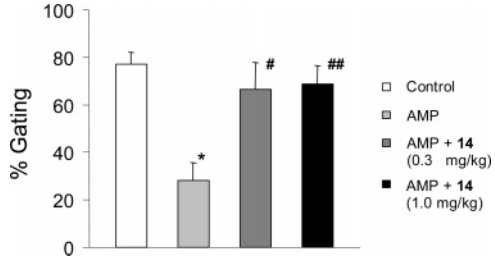

Figure 3. Effect of **14** (0.3 and 1 mg/kg, iv) on the auditory gating deficit in amphetamine treated rats: (∗) $p < 0.001$ vs control ($n = 8$); (#) $p < 0.02$ vs amphetamine (AMP) ($n = 6$), (##) $p < 0.005$ vs AMP ($n = 5$).

auditory gating (corresponding to human P50 auditory gating) in anesthetized rats because of a combination of simultaneous decreases of conditioning responses with corresponding increases in test responses.[37] Subsequent administration of the α7 nAChR agonist **14** (iv, 0.3 or 1 mg/kg) significantly reverses the amphetamine-induced gating deficit (Figure 3). In contrast, application of vehicle in control rats did not normalize amphetamine-induced gating deficit (from 47 ± 5.5% to 41 ± 6.8% gating, $n = 9$). In a separate experiment, **14** at a higher dose (iv, 10 mg/kg) also significantly improves auditory gating given subsequently to amphetamine administration (from 51 ± 3.9% to 68 ± 3.9% gating, $n = 16$, $p < 0.005$). Brain concentrations after 1 and 10 mg/kg, iv administrations of the agonist were 0.56 ± 0.039 nM and 14.9 ± 1.4 μM, respectively, indicating efficacy of **14** on auditory gating at a broad brain exposure range. It has been shown in preclinical studies that α7 nAChR agonists effectively restore pharmacologically, genetically, or environmentally induced gating deficits.[11,12,38]

The potential for **14** to influence learning and memory was evaluated using the rat novel object recognition (NOR) task.[39] This test is based on the ethological observation that rats spend more time exploring objects they have never seen (novel object) than objects that they have recently been exposed to. As with the effect of time on memory in humans, the ability of rats to discriminate between a novel and familiar object diminishes with time following the initial presentation of the familiar object and is lost by 24 h (see vehicle control group of Figure 4). Previous studies have shown that agents with memory-enhancing properties such as acetylcholinesterase inhibitors can prolong the duration that rats will differentially interact with a novel and familiar object.[40] Therefore, **14** was tested in this model by delivering it to rats subcutaneously 30 min before each of the three experimental sessions (see Experimental Section for details). As illustrated in Figure 4, 1 mg/kg of **14** significantly improves the ability of the test subjects to discriminate between the novel and familiar objects following a 24 h delay. While the minimal effective dose of 1 mg/kg cannot be directly compared to the auditory gating model because of the different routes of administration used (iv versus sc), the results from the two models are in good overall agreement. Moreover, the data from these two in vivo models provide evidence that **14** positively influences sensory gating and memory, both of which are believed to be disrupted in patients with schizophrenia.

Conclusion

The synthesis, SAR, and in vitro and in vivo profiles of quinuclidinyl 6,5-fused heteroarylcarboxamides as agonists of the α7 nAChR have been described. Of the 6,5-fused heterocycles evaluated, the furopyridine **14** (PHA-543613) proved to be a potent, high-affinity agonist of the α7 nAChR. The excellent in vitro profile of this compound is matched by rapid

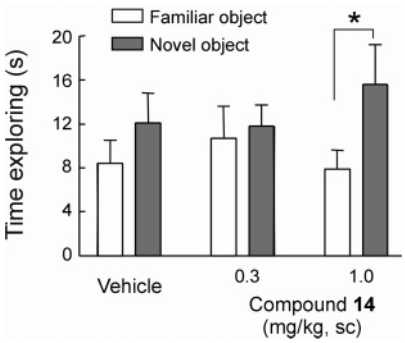

Figure 4. Compound **14** improves performance in the rat novel object recognition (NOR) task: (∗) $p < 0.05$.

brain penetration, high oral bioavailability in rat, and a favorable hERG profile. Furthermore, **14** demonstrates efficacy in two in vivo models, the reversal of an amphetamine-induced P50 gating deficit, and improved performance in a novel object recognition test. The results with this compound provide additional support for the hypothesis that α7 nAChR agonists represent a novel, potential pharmacotherapy to treat the cognitive deficits in schizophrenia.

Experimental Section

Chemistry. Proton (^{1}H) and carbon (^{13}C) nuclear magnetic resonance (NMR) spectra were recorded on a Bruker 400 spectrometer. Chemical shifts are reported in parts per million (δ) relative to tetramethylsilane (δ 0.0). Infrared (IR) spectra, high-resolution mass spectra, and combustion analyses were performed in-house by Structural, Analytical and Medicinal Chemistry Department personnel, Kalamazoo, MI. Melting points were obtained on a Thomas-Hoover melting point apparatus and are uncorrected. Reactions were monitored by thin-layer chromatography (TLC) using Analtech silica gel GF 250 μm plates. The plates were visualized by UV inspection or I_2 stain. Flash chromatography was performed as described by Still[41] using EM Science silica gel 60 (230−400 mesh). All reagents were purchased from either the Aldrich Chemical Co. or The Lancaster Synthesis Co. and used without further purification unless otherwise stated. HATU[42] was purchased from Biosystems, Warrington, U.K. All solvents were HPLC grade unless otherwise stated. Anhydrous solvents were purchased from the Aldrich Chemical Co. and used without further drying.

***N*-[(3*R*)-1-Azabicyclo[2.2.2]oct-3-yl]indole-5-carboxamide (7).** The preparation of racemic compound **7** has been previously described in the literature.[43] Compound **7** was prepared in a similar manner, except 3-(*R*)-aminoquinuclidine was used in place of racemic 3-aminoquinuclidine.

***N*-[(3*R*)-1-Azabicyclo[2.2.2]oct-3-yl]indoline-5-carboxamide (8).** To a stirred solution of indoline-5-carboxylic acid (242 mg, 1.48 mmol) in anhydrous *N*,*N*-dimethylformamide (15 mL) were added diisopropylethylamine (1.0 mL, 5.75 mmol) and 3-(*R*)-aminoquinuclidine dihydrochloride (295 mg, 1.48 mmol). The mixture was cooled to 0 °C, and HATU (562 mg, 1.48 mmol) was added in one portion. The reaction mixture was allowed to warm to room temperature and was stirred overnight. The solvent was removed in vacuo, and the residue was partitioned between saturated aqueous potassium carbonate solution and chloroform. The aqueous layer was extracted with chloroform (3×). The combined organic layers were dried over anhydrous magnesium sulfate, filtered, and concentrated in vacuo. The crude product was purified by flash chromatography on silica gel. Elution with chloroform/methanol/ammonium hydroxide (89:10:1) gave 278 mg (69%) of **8** as a light-pink solid: mp 75−85 °C (color change); $[\alpha]^{25}_D$ 33 (*c* 0.68, MeOH); IR (diffuse reflectance) 3297, 2939, 2868, 1610, 1583, 1532, 1494, 1473, 1456, 1323, 1265, 1201, 1055, 766, 616 cm^{-1}; ^{1}H NMR (400 MHz, $CDCl_3$) δ 7.61 (s, 1H), 7.55 (d, $J = 8.3$ Hz, 1H), 6.61 (d, $J = 8.3$ Hz, 1H), 6.28 (d, $J = 6.2$ Hz, 1H), 4.23−4.17 (m, 1H),

4.08 (s, 1H), 3.68 (t, $J = 8.4$ Hz, 2H), 3.51−3.45 (m, 1H), 3.11 (t, $J = 8.4$ Hz, 2H), 3.06−3.02 (m, 1H), 2.98−2.87 (m, 3H), 2.78−2.73 (m, 1H), 2.11−2.09 (m, 1H), 1.88−1.75 (m, 3H), 1.61−1.53 (m, 1H); ^{13}C NMR (100 MHz, $CDCl_3$) δ 167.7, 154.8, 129.1, 127.6, 123.9, 123.8, 107.7, 54.49, 47.38, 47.17, 46.60, 46.22, 29.13, 25.52, 24.61, 19.50; high-resolution MS (FAB) calcd for $C_{16}H_{22}N_3O$ [M + H] *m/e* 272.1763, found 272.1758.

***N*-[(3*R*)-1-Azabicyclo[2.2.2]oct-3-yl]-1-benzothiophene-5-carboxamide Fumarate (9).** To a stirred solution of 1-benzothiophene-5-carboxylic acid[44] (178 mg, 1.0 mmol) in anhydrous *N*,*N*-dimethylformamide (12 mL) were added diisopropylethylamine (522 μL, 3.00 mmol) and 3-(*R*)-aminoquinuclidine dihydrochloride (190 mg, 0.95 mmol). The mixture was cooled to 0 °C, and HATU (361 mg, 0.95 mmol) was added in one portion. The reaction mixture was allowed to warm to room temperature and was stirred overnight. The solvent was removed in vacuo, and the residue was partitioned between half-saturated aqueous potassium carbonate solution and chloroform/methanol (9:1). The aqueous layer was extracted with 9:1 chloroform/methanol (2×), and the combined organic layers were washed with brine, dried over anhydrous sodium sulfate, filtered, and concentrated in vacuo. The crude product was purified by flash chromatography on silica gel. Elution with chloroform/methanol/ammonium hydroxide (89:9:1) gave 256 mg (90%) of a white foam. The foam (256 mg, 0.89 mmol) was dissolved in acetone (5 mL), and a hot solution of fumaric acid (109 mg, 0.93 mmol) in methanol (20 mL) was added. The mixture was stirred for 15 min at 45 °C. The solvent was removed in vacuo, and the remaining residue was diluted with acetone (10 mL) and water (0.2 mL). The mixture was stirred overnight at room temperature. The solid was collected by filtration, washed with acetone, and dried under high vacuum overnight to give 260 mg (71%) of **9** as a white solid: mp 120−123 °C; $[\alpha]^{25}_D$ 11 (*c* 0.62, H_2O); IR (diffuse reflectance) 3424, 3346, 3224, 3101, 3060, 3044, 2972, 1699, 1663, 1628, 1555, 1539, 1487, 1288, 1253 cm^{-1}; ^{1}H NMR (400 MHz, MeOH-d_4) δ 8.40 (d, 1H, $J = 1.30$ Hz), 8.03 (d, 1H, $J = 8.47$ Hz), 7.84 (dd, 1H, $J = 8.47$, 1.60 Hz), 7.71 (d, 1H, $J = 5.46$ Hz), 7.50 (d, 1H, $J = 5.45$ Hz), 6.71 (s, 2H), 4.50−4.45 (m, 1H), 3.90−3.82 (m, 1H), 3.52−3.28 (m, 5H), 2.40−2.36 (m, 1H), 2.33−2.21 (m, 1H), 2.16−2.08 (m, 2H), 2.01−1.90 (m, 1H); ^{13}C NMR (100 MHz, MeOH-d_4) δ 171.8, 171.5, 144.9, 141.3, 136.6, 131.8, 129.8, 125.7, 124.5, 124.4, 123.9, 53.70, 47.91, 47.46, 47.20, 26.22, 23.31, 18.96; high-resolution MS (FAB) calcd for $C_{16}H_{19}N_2OS$ [M + H] *m/e* 287.1218, found 287.1227; % water (KF), 3.74.

***N*-[(3*R*)-1-Azabicyclo[2.2.2]oct-3-yl]-1-benzothiophene-6-carboxamide Fumarate (10).** To a stirred solution of 1-benzothiophene-6-carboxylic acid (178 mg, 1.0 mmol) in anhydrous *N*,*N*-dimethylformamide (10 mL) were added diisopropylethylamine (522 μL, 3.00 mmol) and 3-(*R*)-aminoquinuclidine dihydrochloride (190 mg, 0.95 mmol). The mixture was cooled to 0 °C, and HATU (361 mg, 0.95 mmol) was added in one portion. The reaction mixture was allowed to warm to room temperature and was stirred overnight. The solvent was removed in vacuo, and the residue was partitioned between half-saturated aqueous potassium carbonate solution and chloroform/methanol (9:1). The aqueous layer was extracted with 9:1 chloroform/methanol (2×), and the combined organic layers were washed with brine, dried over anhydrous sodium sulfate, filtered, and concentrated in vacuo. The crude product was purified by flash chromatography on silica gel. Elution with chloroform/methanol/ammonium hydroxide (89:9:1) gave 260 mg (95%) of a white solid. The solid (260 mg, 0.91 mmol) was dissolved in methanol (3 mL), and fumaric acid (105 mg, 0.91 mmol) was added. The mixture was stirred for 15 min at 45 °C. The solvent was removed in vacuo and the remaining residue was diluted with acetone (10 mL) and water (0.1 mL). The mixture was stirred overnight at room temperature. The solid precipitate was collected by filtration, washed with acetone, and dried under high vacuum overnight to give 260 mg (71%) of **10** as a white solid: mp 124−127 °C (loss of H_2O); IR (diffuse reflectance) 3423, 3225, 3060, 3012, 2965, 1703, 1628, 1555, 1486, 1464, 1324, 1290, 1276, 1250, 787 cm^{-1}; ^{1}H NMR (400 MHz, MeOH-d_4) δ 8.48 (s, 1H), 7.95 (d, 1H, $J = 8.36$ Hz), 7.87 (dd, 1H, $J = 8.37$, 1.54 Hz), 7.80 (d, 1H, $J = 5.45$ Hz), 7.48 (d, 1H, $J = 5.44$ Hz), 6.71 (s, 2H), 4.52−4.45 (m, 1H), 3.89−3.80 (m, 1H), 3.50−3.25 (m, 5H), 2.41−2.36 (m, 1H), 2.33−2.23 (m, 1H), 2.15−2.08 (m, 2H), 2.00−1.88 (m, 1H); ^{13}C NMR (100 MHz, MeOH-d_4) δ 171.8, 171.2, 144.1, 141.4, 136.6, 131.6, 131.4, 125.3, 125.0, 124.8, 123.6, 53.73, 47.92, 47.47, 47.23, 26.21, 23.32, 18.97; high-resolution MS (FAB) calcd for $C_{16}H_{19}N_2OS$ [M + H] *m/e* 287.1218, found 287.1222; % water (KF), 4.57.

***N*-[(3*R*)-1-Azabicyclo[2.2.2]oct-3-yl]-2,3-dihydro-1-benzofuran-5-carboxamide Fumarate (12).** To a stirred solution of 2,3-dihydrobenzofuran-5-carboxylic acid (300 mg, 1.8 mmol) and 3-(*R*)-aminoquinuclidine dihydrochloride (346 mg, 1.7 mmol) in *N*,*N*-dimethylformamide (18 mL) was added diisopropylethylamine (960 μL, 5.5 mmol). The solution was stirred for 10 min, followed by cooling with an ice bath. HATU (660 mg, 1.7 mmol) was added, and the mixture was allowed to warm to room temperature and was stirred for 16 h. The solvent was removed in vacuo, and the remaining residue was partitioned between saturated aqueous potassium carbonate solution and chloroform/methanol (9:1). The aqueous layer was extracted with 9:1 chloroform/methanol, and the combined organic layers were washed with brine, dried over anhydrous magnesium sulfate, filtered, and concentrated in vacuo to a clear residue. The residue was purified by flash chromatography on silica gel. Elution with chloroform/methanol/ammonium hydroxide (92:7:1) gave 470 mg (99%) of a white foam. The foam (470 mg, 1.7 mmol) was taken up in acetone (10.0 mL), and a hot solution of fumaric acid (200 mg, 1.7 mmol) in isopropyl alcohol was added. The mixture was warmed in a water bath to 45 °C for 15 min, followed by removal of the solvent in vacuo. The residue was triturated in acetone (3.0 mL), filtered, and dried in vacuo to afford 630 mg (94%) of **12** as a white solid: mp 138−142 °C; $[\alpha]^{25}_D$ 4 (*c* 0.89, MeOH); IR (diffuse reflectance) 3417, 3231, 2986, 2971, 1705, 1664, 1621, 1551, 1487, 1324, 1315, 1293, 1285, 1241, 784 cm^{-1}; ^{1}H NMR (400 MHz, MeOH-d_4) δ 7.77 (s, 1H), 7.69 (d, 1H, $J = 8.40$ Hz), 6.81 (d, 1H, $J = 8.38$ Hz), 6.70 (s, 2H), 4.65 (t, 2H, $J = 8.76$ Hz), 4.43−4.37 (m, 1H), 3.84−3.78 (m, 1H), 3.42−3.30 (m, 4H), 3.28 (t, 1H, $J = 8.74$ Hz), 3.24−3.18 (m, 1H), 2.35−2.32 (m, 1H), 2.27−2.19 (m, 1H), 2.11−2.05 (m, 2H), 1.97−1.88 (m, 1H); ^{13}C NMR (100 MHz, MeOH-d_4) δ 171.5, 170.7, 164.9, 136.3, 129.7, 129.2, 127.3, 125.8, 109.8, 73.19, 53.47, 47.57, 47.12, 46.70, 30.06, 25.85, 22.96, 18.59; high-resolution MS (FAB) calcd for $C_{16}H_{21}N_2O_2$ [M + H] *m/e* 273.1603, found 273.1597; % water (KF), 4.48.

***N*-[(3*R*)-1-Azabicyclo[2.2.2]oct-3-yl]-1-benzofuran-5-carboxamide Fumarate (11).** To a stirred solution of benzofuran-5-carboxylic acid (2.0 g, 12.3 mmol) in anhydrous *N*,*N*-dimethylformamide (100 mL) were added diisopropylethylamine (6.4 mL, 36.9 mmol) and 3-(*R*)-aminoquinuclidine dihydrochloride (2.33 g, 11.7 mmol). The mixture was cooled to 0 °C, and HATU (4.46 g, 11.7 mmol) was added in one portion. The reaction mixture was allowed to warm to room temperature and was stirred for 36 h. The solvent was removed in vacuo, and the residue was partitioned between half-saturated aqueous potassium carbonate solution and chloroform/methanol (9:1). The aqueous layer was extracted with 9:1chloroform/methanol (2×). The combined organic layers were washed with brine, dried over anhydrous magnesium sulfate, filtered, and concentrated in vacuo. The crude product was purified by flash chromatography on silica gel. Elution with chloroform/methanol/ammonium hydroxide (89:9:1) gave 1.09 g (97%) of a white solid. The solid 2.77 g (10.2 mmol) was dissolved in methanol (30 mL), and fumaric acid (1.19 g, 10.2 mmol) was added. The mixture was warmed to 50 °C for 30 min. The solvent was removed in vacuo, and the remaining residue was diluted with acetone (50 mL). The mixture was stirred overnight at room temperature. The solid precipitate was collected by filtration, washed with acetone, and dried under high vacuum overnight to give 3.63 g (92%) of **11** as a white solid: mp 120−130 °C (loss of H_2O); $[\alpha]^{25}_D$ 6 (*c* 1.04, MeOH); IR (mull) 3422, 3229, 1627, 1614, 1555, 1488, 1438, 1292, 1262, 1138, 1108, 1101, 1026, 901, 786 cm^{-1}; ^{1}H NMR (400 MHz, MeOH-d_4) δ 8.20 (s, 1H), 7.88 (d, 1H, $J = 2.06$ Hz), 7.85 (dd,

1H, J = 8.66, 1.74 Hz), 7.61 (d, 1H, J = 8.62 Hz), 6.97 (d, 1H, J = 1.26 Hz), 6.70 (s, 2H), 4.50−4.43 (m, 1H), 3.89−3.80 (m, 1H), 3.50−3.23 (m, 5H), 2.40−2.34 (m, 1H), 2.32−2.21 (m, 1H), 2.16−2.08 (m, 2H), 2.00−1.89 (m, 1H); ^{13}C NMR (100 MHz, MeOH-d_4) δ 171.8, 171.5, 158.6, 148.6, 136.6, 130.6, 129.4, 125.5, 122.7, 112.6, 108.4, 53.77, 47.92, 47.47, 47.20, 26.20, 23.31, 18.96; high-resolution MS (FAB) calcd for $C_{16}H_{19}N_2O_2$ [M + H] *m*/*e* 271.1446, found 271.1450; % water (KF), 4.48.

***N*-[(3*R*)-1-Azabicyclo[2.2.2]oct-3-yl]-1-benzofuran-6-carboxamide Hydrochloride (13).** 1-Benzofuran-6-carboxylic acid (162 mg, 1.0 mmol) was combined with (*R*)-3-aminoquinuclidine dihydrochloride (219 mg, 1.1 mmol), diisopropylethylamine (522 μL, 3.0 mmol), and DMF (5 mL), cooled to 0 °C, and treated with HATU (380 mg, 1.0 mmol). The mixture was allowed to warm to room temperature and was stirred for 18 h. The mixture was concentrated in vacuo and partitioned between a 1:1 mixture of saturated sodium chloride/concentrated ammonium hydroxide (10 mL) and chloroform (30 mL). The aqueous layer was extracted with chloroform. The organics were combined, dried over anhydrous sodium sulfate, and concentrated to an amber oil (530 mg). The crude material was chromatographed over 11 g of slurry-packed silica gel, eluting with 2% ammonium hydroxide/10% methanol/chloroform into 7 mL fractions. Fractions 3−6 were combined and concentrated to a dark-yellow solid (274 mg). The solid was further dried in vacuo. The solid was dissolved in methanol (5 mL), treated with 3 N methanolic hydrochloric acid (1 mL), stirred for 16 h, then concentrated to dryness. The residue was dissolved in methanol (1 mL) and 2-propanol (10 mL) and treated with diethyl ether (~20 mL) until the mixture became turbid. The mixture was stirred for 16 h, filtered under nitrogen, and dried in a vacuum oven at 50 °C to afford 206 mg (67%) of **13** as an off-white solid. IR (diffuse reflectance) 3245, 2663, 2640, 2550, 2490, 1650, 1538, 1318, 1311, 1277, 839, 831, 775, 733, 624 cm^{-1}; ^{1}H NMR (400 MHz, D_2O) δ 1.86 (m, 1 H), 1.99 (m, 2 H), 2.12 (m, 1 H), 2.27 (m, 1 H), 3.15−3.33 (m, 5 H), 3.73 (m, 1 H), 4.29 (m, 1 H), 6.85 (d, J = 2 Hz, 1 H), 7.52 (d, J = 8 Hz, 1 H), 7.63 (d, J = 8 Hz, 1 H), 7.79 (d, J = 2 Hz, 1 H), 7.81 (s, 1 H); ^{13}C NMR (125 MHz, D_2O) δ 17.27, 21.55, 24.23, 45.77, 46.43, 46.84, 52.41, 107.13, 111.04, 121.82, 122.32, 129.53, 131.42, 148.70, 154.29, 171.67; high-resolution MS (FAB) calcd for $C_{16}H_{18}N_2O_2$ [M + H] *m*/*e* 271.1446, found 271.1447; % water (KF), 0.48.

***N*-[(3*R*)-1-Azabicyclo[2.2.2]oct-3-yl]furo[2,3-*c*]pyridine-5-carboxamide Dihydrochloride (14).** Furo[2,3-*c*]pyridine-5-carboxylic acid (5.0 g, 25 mmol) was combined with diisopropylethylamine (20.9 mL, 120 mmol) and (*R*)-3-aminoquinuclidine dihydrochloride (5.97 g, 30 mmol) in DMF (125 mL), cooled to 0 °C, and treated with HATU (11.4 g, 30 mmol). The mixture was allowed to warm to room temperature and was stirred for 3 h, then concentrated under high vacuum to near-dryness. The resulting residue was dissolved in 10% methanol/chloroform (400 mL) and washed with 1:1 saturated brine/concentrated ammonium hydroxide (200 mL), and the aqueous layer was extracted with 5% methanol/chloroform (2 × 100 mL). The combined organics were dried over potassium carbonate and concentrated to a tan solid. The crude material was chromatographed over 250 g slurry-packed silica gel, eluting with 0.5% ammonium hydroxide/8% methanol/chloroform into a 500 mL forerun, followed by 50 mL fractions. NOTE: Methylene chloride should be avoided during chromatography as we have observed that quinuclidine **14**, as well as other similar quinuclidine-containing compounds, is reactive toward methylene chloride and results in the formation of a quaternary salt. Fractions 14−54 were combined and concentrated to a tan solid. The resulting solid was dissolved in methanol and treated with 1 N hydrochloric acid in methanol (60.0 mL). The material was concentrated to dryness, then stirred overnight in methanol (50 mL) and isopropanol (50 mL). The resulting solid was collected under nitrogen and dried in a vacuum oven without heat to afford 8.1 g (94%) of **14** as a white solid: mp 313−315 °C; IR (diffuse reflectance) 3157, 3084, 2959, 2932, 2794, 2671, 2644, 2626, 2365, 2015, 1678, 1553, 1479, 1451, 1206 cm^{-1}; ^{1}H NMR (300 MHz, D_2O) δ 1.90 (m, 1 H), 2.03 (m, 2 H), 2.18 (m, 1 H), 2.36 (m, 1 H), 3.25−3.40 (m, 5 H), 3.78 (m, 1 H), 4.44 (m, 1 H), 7.16 (s, 1 H), 8.19 (s, 1 H), 8.47 (s, 1 H), 8.96 (s, 1 H); ^{13}C NMR (100 MHz, D_2O) δ 17.25, 21.55, 24.29, 45.75, 46.47, 46.89, 52.17, 108.09, 117.74, 131.20, 138.86, 139.71, 153.09, 154.24, 165.46; low resolution MS (ESI) *m*/*e* 271 [M$^+$].

***N*-[(3*R*)-1-Azabicyclo[2.2.2]oct-3-yl]furo[2,3-*b*]pyridine-5-carboxamide Dihydrochloride (15).** Furo[2,3-*b*]pyridine-5-carboxylic acid (359 mg, 2.2 mmol) and triethylamine (307 μL, 2.2 mmol) were suspended in methylene chloride (10 mL), stirred until dissolved, treated with diphenylphosphorylazide (431 μL, 2.0 mmol), and stirred for 20 min. The solution was treated with (*R*)-3-aminoquinuclidine (252 mg, 2.0 mmol) in methylene chloride (3 mL) and stirred for 18 h at ambient temperature. The solution was diluted with methanol and loaded onto a column of AG 50W-X2 resin (hydrogen form). The column was rinsed with methanol, and the product eluted with a 5% triethylamine/methanol solution onto a column of AMBERJET 4400 OH resin. The eluted material was concentrated to an oil. The crude material was chromatographed over 25 g of slurry-packed silica gel, eluting with 0.5% ammonium hydroxide/5% methanol/methylene chloride and then 0.5% ammonium hydroxide/8% methanol/methylene chloride and finally 2% ammonium hydroxide/15% methanol/methylene chloride into 7 mL fractions. Fractions 45−72 were collected and concentrated to an oil. The oil was dissolved in 2 mL of methanol and treated with 1 N hydrochloric acid in methanol (2.24 mL). The material was concentrated to dryness, treated with 10% methylene chloride/45% ether/ethyl acetate, and stirred for several hours. The resulting solid was collected under nitrogen to afford 147 mg (21.4%) of **15** as a white solid: mp 109−110 °C; IR (diffuse reflectance) 3251, 3241, 2350, 2334, 2318, 2050, 1990, 1662, 1656, 1645, 1550, 1536, 1378, 776, 770 cm^{-1}; ^{1}H NMR (300 MHz, DMSO-d_6) δ 1.92 (m, 1 H), 2.08 (m, 2 H), 2.33 (m, 2 H), 3.55−3.66 (m, 5 H), 3.98 (m, 1 H), 4.44 (m, 1 H), 7.16 (d, J = 2 Hz, 1 H), 8.23 (d, J = 2 Hz, 1 H), 8.69 (d, J = 2 Hz, 1 H), 8.86 (d, J = 2 Hz, 1 H), 9.15 (d, J = 3 Hz, 1 H); high-resolution MS (FAB) calcd for $C_{15}H_{18}N_3O_2$ [M + H] *m*/*e* 272.1399, found 272.1409.

***N*-[(3*R*)-1-Azabicyclo[2.2.2]oct-3-yl]furo[3,2-*c*]pyridine-6-carboxamide Dihydrochloride (16).** Methylfuro[3,2-*c*]pyridine 6-carboxylate (141 mg, 0.796 mmol) was combined with aqueous sodium hydroxide (3 N solution, 534 μL, 1.75 mmol) in methanol (3 mL) and water (1.5 mL) and stirred at room temperature for 7 h. The reaction mixture was concentrated to dryness. The remaining residue was combined with diisopropylethylamine (610 μL, 3.50 mmol), (*R*)-3-aminoquinuclidine dihydrochloride (174 mg, 0.876 mmol), and DMF (6 mL) and cooled to 0 °C. HATU (333 mg, 0.876 mmol) was added, and the mixture was allowed to warm to room temperature and was stirred for 2 h. The reaction mixture was concentrated to dryness and chromatographed over 10 g of slurry-packed silica gel, eluting with 0.5% ammonium hydroxide/10% methanol/chloroform into 7 mL fractions. Fractions 4−18 were combined and concentrated in vacuo to an oil that contained an impurity from the diisopropylethylamine based on the ^{1}H NMR spectra. The oil was stirred vigorously with 1:1 saturated brine/ammonium hydroxide (25 mL), extracted with 5% methanol/chloroform (25 mL), and washed with 1:1 saturated brine/ammonium hydroxide (20 mL), and the combined aqueous layers were back-extracted with 5% methanol/chloroform (25 mL). The combined organics were dried over sodium sulfate and concentrated to a yellow oil (160 mg). The oil was dissolved in methanol (500 μL), treated with 3 M hydrochloric acid in methanol (492 μL), and stirred for 18 h. The resulting solid was filtered under nitrogen and dried in a vacuum oven at 50 °C for 6 h to afford 91 mg (33%) of **16** as a white solid: IR (diffuse reflectance) 3139, 3101, 3067, 3025, 2989, 2962, 2551, 2532, 2515, 2505, 2455, 1668, 1520, 1451, 1329 cm^{-1}; ^{1}H NMR (400 MHz, D_2O) δ 1.87 (m, 1 H), 2.00 (m, 2 H), 2.15 (m, 1 H), 2.33 (m, 1 H), 3.21−3.34 (m, 5 H), 3.75 (m, 1 H), 4.42 (m, 1 H), 7.14 (s, 1 H), 8.06 (s, 1 H), 8.37 (s, 1 H), 9.02 (s, 1 H); ^{13}C NMR ($CDCl_3$) δ 17.22, 21.51, 24.25, 45.83, 46.44, 46.85, 52.07, 106.60, 108.46, 128.60, 141.22, 141.45, 151.67, 161.29, 164.78; high-resolution MS (FAB) calcd for $C_{15}H_{18}N_3O_2$ [M + H] *m*/*e* 272.1399, found 272.1390.

(*R*)-*N*-(Quinuclidin-3-yl)furo[2,3-*b*]pyridine-6-carboxamide (17). To a stirred solution of furo[2,3-*b*]pyridine-6-carboxylic acid[45] (0.12 g, 0.78 mmol) in anhydrous *N*,*N*-dimethylformamide (3 mL) were added triethylamine (0.33 mL, 2.3 mmol) and 3-(*R*)-aminoquinuclidine dihydrochloride (0.15 g, 0.78 mmol). The mixture was cooled to 0 °C, and HATU (0.30 g, 0.78 mmol) was added in one portion. The reaction mixture was allowed to warm to room temperature and was stirred for 24 h. The crude product was worked up by loading onto a column of AG Dowex resin (50-X2). After the column was washed with methanol (three column volumes), the product was eluted with methanol/triethylamine (95:5) and the fractions containing the product were concentrated to afford an orange solid. The solid was partitioned between a 50:50 mixture of acetonitrile and methanol and filtered to afford 0.08 g (88%) of **17** as a light-brown solid: IR (liq) 2940, 2868, 1995, 1934, 1670, 1587, 1516, 1455, 1404, 1355, 1271, 1133, 1056, 748 cm^{-1}; ^1H NMR (400 MHz, DMSO-d_6) δ 8.56 (d, 1H, $J = 2.55$ Hz), 8.29 (d, 1H, $J = 8.84$ Hz), 8.03 (d, 1H, $J = 2.55$), 7.15 (d, 1H, $J = 8.84$ Hz), 4.06−3.91 (m, 1H), 3.21−3.05 (m, 1H), 3.02−2.85 (m, 1H), 2.85−2.58 (m, 4H), 1.94−1.84 (m, 1H), 1.83−1.71 (m, 1H), 1.68−1.54 (m, 2H), 1.42−1.27 (m, 1H); high-resolution MS (ESI) calcd for $C_{15}H_{17}N_3O_2$ [M + H] *m*/*e* 272.1399, found 272.1407; % water (KF), 5.62.

***N*-[(3*R*)-1-Azabicyclo[2.2.2]oct-3-yl]thieno[2,3-*c*]pyridine-5-carboxamide Dihydrochloride (18).** Thieno[2,3-*c*]pyridine-5-carboxylic acid (189 mg, 1.05 mmol) was combined with triethylamine (0.167 mL, 1.20 mmol) in methylene chloride (4 mL). Bis(2-oxo-3-oxazolidinyl)phosphinic chloride (311 mg, 1.22 mmol) was added portionwise, and the solution was stirred at room temperature for 30 min. A 0.5 M free-based (*R*)-3-aminoquinuclidine solution in DMF (3 mL, 1.5 mmol) was added dropwise, and the mixture was stirred for 4 h. The reaction mixture was poured through prewashed Amberjet 4400 OH strongly basic anion exchanger resin directly onto prewashed AG 50W-X2 hydrogen form resin. The acid resin was washed with methanol (100 mL), and the product was eluted with 10% triethylamine/methanol solution (100 mL). The solution was concentrated in vacuo to a glass. The crude material was chromatographed over 10 g of slurry-packed silica gel, eluting with 1% ammonium hydroxide/10% methanol/methylene chloride into 100 mm fractions. Fractions 7−15 were collected and concentrated in vacuo to yield 0.115 g (38%) of glass. The glass was dissolved in 1 M hydrochloric acid in methanol (1.6 mL) and was stirred for 2 h. Isopropyl alcohol (2 mL) and ether (4 mL) were added to enhance precipitation. The precipitate was isolated via filtration and dried to afford 120 mg (32%) of **18** as a white solid: mp 300−301 °C; IR (diffuse reflectance) 3040, 2965, 2938, 2884, 2843, 2770, 2479, 2351, 2334, 2318, 2022, 1667, 1578, 1551, 1517, cm^{-1}; ^1H NMR (400 MHz, D_2O) δ 1.91 (m, 1 H), 2.03 (m, 2 H), 2.19 (m, 1 H), 2.36 (m, 1 H), 3.31 (m, 5 H), 3.79 (m, 1 H), 4.45 (m, 1 H), 7.67 (d, $J = 5$ Hz, 1 H), 8.28 (d, $J = 5$ Hz, 1 H), 8.57 (s, 1 H), 9.25 (s, 1 H); ^{13}C NMR (125 MHz, D_2O) δ 17.25, 21.53, 24.29, 45.77, 46.46, 46.88, 52.13, 118.69, 124.81, 139.38, 140.54, 142.02, 148.19, 165.36; % water (KF), 5.94.

***N*-[(3*R*)-1-Azabicyclo[2.2.2]oct-3-yl]thieno[3,2-*c*]pyridine-6-carboxamide Dihydrochloride (19).** Thieno[3,2-*c*]pyridine-6-carboxylic acid (185 mg, 1.03 mmol) was combined with triethylamine (0.167 mL, 1.20 mmol) in methylene chloride (4 mL). Bis(2-oxo-3-oxazolidinyl)phosphinic chloride (308 mg, 1.20 mmol) was added portionwise, and the solution was stirred at room temperature for 30 min. A 0.5 M free-based (*R*)-3-aminoquinuclidine solution in DMF (3 mL, 1.5 mmol) was added dropwise, and the mixture was stirred for 4 h. The reaction mixture was poured through prewashed Amberjet 4400 OH strongly basic anion exchanger resin directly onto prewashed AG 50W-X2 hydrogen form resin. The acid resin was washed with methanol (100 mL), and the product eluted with 10% triethylamine/methanol solution (100 mL). The solution was concentrated in vacuo to a glass. The crude material was chromatographed over 10 g of slurry-packed silica gel, eluting with 1% ammonium hydroxide/10% methanol/methylene chloride into 100 mm fractions. Fractions 6−14 were collected and concentrated in vacuo to yield 0.115 g (39%) of glass. The glass was dissolved in 1 M hydrochloric acid in methanol (1.6 mL) and stirred for 2 h. Isopropyl alcohol (2 mL) and ether (4 mL) were added to enhance precipitation. The precipitate was isolated via filtration and dried to afford 116 mg (31%) of **19** as a white solid: mp 294−295 °C; IR (diffuse reflectance) 3067, 2961, 2931, 2802, 2793, 2674, 2626, 2609, 2472, 2463, 2350, 2329, 2196, 1670, 1551, cm^{-1}; ^1H NMR (400 MHz, D_2O) δ 1.91 (m, 1 H), 2.03 (m, 2 H), 2.17 (m, 1 H), 2.36 (m, 1 H), 3.29 (m, 5 H), 3.79 (m, 1 H), 4.45 (m, 1 H), 7.73 (d, $J = 6$ Hz, 1 H), 8.05 (d, $J = 5$ Hz, 1 H), 8.78 (s, 1 H), 9.16 (s, 1 H); ^{13}C NMR (125 MHz, D_2O) δ 16.47, 20.37, 23.49, 45.07, 45.67, 46.09, 51.31, 118.21, 123.15, 134.88, 136.23, 137.34, 141.05, 151.22, 163.90; high-resolution MS (FAB) calcd for $C_{15}H_{18}N_3OS$ [M + H] *m*/*e* 288.1170, found 288.1174; % water (KF), 3.37.

***N*-[(3*R*)-1-Azabicyclo[2.2.2]oct-3-yl]-1*H*-pyrrolo[2,3-*c*]pyridine-5-carboxamide Dihydrochloride (20).** 1*H*-Pyrrolo[2,3-*c*]pyridine-5-carboxylic acid (250 mg, 1.54 mmol) was combined with diisopropylethylamine (0.80 mL, 4.6 mmol) and (*R*)-(3)-aminoquinuclidine dihydrochloride (309 mg, 1.55 mmol) in tetrahydrofuran (8 mL) and cooled in an ice bath. HATU (586 mg, 1.54 mmol) was added portionwise, and the mixture was stirred for 7 h at room temperature. Saturated $NaHCO_3$ (10 mL) was added, and the mixture was stirred overnight. The reaction mixture was diluted with CH_2Cl_2 (16 mL), and the organic was rinsed with 1 M NaOH (1 × 10 mL). The organics were dried over $MgSO_4$, filtered, and concentrated to a pale oil. The crude material was chromatographed over 12 g of slurry-packed silica, eluting with 1% concentrated NH_4OH/10% MeOH/CH_2Cl_2. The appropriate fractions were collected and concentrated to a pale oil. The oil was dissolved in 1 M HCl in methanol (3 mL) and stirred for 1.5 h. Isopropyl alcohol (4 mL) was added, and ether was dripped in until a precipitate formed. Following another 1 h of stirring, the precipitate was isolated via filtration and washed with ether, affording 212 mg (40%) of *N*-[(3*R*)-1-azabicyclo[2.2.2]oct-3-yl]-1*H*-pyrrolo[2,3-*c*]pyridine-5-carboxamide dihydrochloride (**20**) as a white solid: IR (diffuse reflectance) 3182, 3160, 3121, 3029, 2999, 2951, 2910, 2874, 2836, 2797, 2351, 2317, 2063, 1672, 1550 cm^{-1}; ^1H NMR (400 MHz, methanol-d_4) δ 9.07 (s, 2H), 8.29 (d, 1H, $J = 2.9$ Hz), 7.17 (d, 1H, $J = 2.9$ Hz), 4.62−4.56 (m, 1H), 3.90−3.72 (m, 1H), 3.65−3.51 (m, 2H), 3.45−3.30 (m, 3H), 2.48−2.42 (m, 1H), 2.41−2.30 (m, 1H), 2.17−2.08 (m, 2H), 2.01−1.90 (m, 1H); ^{13}C NMR (125 MHz, methanol-d_4) δ 161.9, 140.0, 137.8, 132.0, 130.5, 128.0, 116.5, 105.6, 51.75, 46.25, 46.03, 24.22, 21.66, 17.63; high-resolution MS (API) calcd for $C_{15}H_{19}N_4O$ [M + H] *m*/*e* 271.1559, found 271.1562; % water (KF), 7.28.

Details of the in Vitro Assays. Reactive Metabolite Assay (RMA). The assay was performed as described previously.[46] Stock solutions of the test compounds were prepared in methanol. The final concentration of methanol in the incubation media was 0.2% (v/v). Incubations were carried out at 37 °C for 60 min in a shaking water bath. The incubation volume was 1 mL and consisted of the following: 0.1 M potassium phosphate buffer (pH 7.4), human liver microsomes (P450 concentration = 0.5 μM), NADPH (1.2 mM), and substrate (200 μM). The reaction mixture was prewarmed at 37 °C for 2 min before adding NADPH. GSH-EE (2 mM) was added 3 min after initiation of the reaction with NADPH. Incubations that lacked either NADPH or GSH-EE served as negative controls, and reactions were terminated by the addition of ice-cold acetonitrile (1 mL). The solutions were centrifuged (3000*g*, 15 min), and the supernatants were dried under a steady nitrogen stream. The residue was reconstituted with mobile phase and analyzed for metabolite formation by liquid chromatography tandem mass spectrometry (LC/MS/MS) as described previously for other xenobiotics.

Human Liver Microsome Stability Assay (HLM). Substrate (final concentration = 1 μM) was incubated in human liver microsomes (HL-mix-101, prepared from 59 individual donors, 0.25 μM P450 final concentration) and 100 mM potassium phosphate buffer (pH 7.4). The reaction was initiated by the addition of an NADPH-generating system (0.5 mM $NADP^+$, 10.5 mM $MgCl_2$,

5.6 mM DL-isocitric acid and 0.5 U/mL isocitric dehydrogenase). Equations used for scaling to in vivo conditions were described previously.[47]

Rat Liver Microsome Stability Assay (RLM). Assay protocol was the same as for HLM assay only rat liver microsomes (RL-mix 142, prepared from female Spraque-Dawley rats) were used during incubation. Equations used for scaling to in vivo conditions were described previously.[47]

Functional High-Throughput Screens for α7 5-HT$_3$ Chimera, 5-HT$_3$, Neuromuscular Junction (α1$\beta_1\gamma\delta$), and Ganglionic (α3β_4) nAChRs. The α7 5-HT$_3$ chimera and the 5-HT$_3$ receptor were stably expressed in SH-EP1 cells. TE671 and SH-SY5Y cells were used as an endogenous source for neuromuscular junction and ganglionic nAChRs, respectively.[48] All functional high-throughput screens were conducted as calcium flux assays using the fluorescence imaging plate reader (FLIPR, Molecular Devices). Transfected SH-EP1 cells were grown in minimal essential medium (MEM) containing nonessential amino acids supplemented with 10% fetal bovine serum, L-glutamine, 100 units/mL penicillin/streptomycin, 250 ng/mL fungizone, 400 μg/mL Hygromycin B, and 800 μg/mL Geneticin. TE671 and SH-SY5Y cells were grown according to published methods. All cells were grown in a 37 °C incubator with 5−6% CO_2. The cells were trypsinized and plated in either 96- or 384-well black/clear assay plates. Cells were loaded in a 1:1 mixture of 2 mM Calcium Green-1 AM (Molecular Probes) prepared in anhydrous dimethyl sulfoxide and 20% pluronic F-127 (Molecular Probes). This reagent was added directly to the growth medium of each well to achieve a final concentration of 2 μM Calcium Green-1 AM. Cells were then incubated in the dye for 1 h at 37 °C and then washed with two cycles in a plate washer. Each cycle was programmed to wash each well four times with Mark's modified Earle's balanced salt solution (MMEBSS) composed of (in mM): $CaCl_2$ (4), $MgSO_4$ (0.8), NaCl (20), KCl (5.3), D-glucose (5.6), Tris-HEPES (20), *N*-methyl-D-glucamine (120), pH 7.4. After the last cycle, the cells were allowed to incubate at 37 °C for at least 10 min in MMEBSS. FLIPR was set up to excite Calcium Green-1 AM at 488 nm using 500−600 mW of power and reading fluorescence emission above 525 nm. A 0.5 or 0.7 s exposure was used to illuminate each well. After 30 s of baseline recording, test compounds were added to each well of the assay plate from a 3 or 4× stock solutions. Agonist responses were evaluated as the signal increase over baseline upon addition of the test compound. Antagonist activity was evaluated in some experiments by adding either nicotine (nAChRs) or serotonin (5-HT$_3$R) 2 min after the test compound was added and measuring the loss of response to the known agonist compared to wells treated with vehicle.

Brain Homogenate Binding Assays ([^{3}H]MLA, [^{3}H]Cytisine,[49] [^{3}H]GR65630). Male Sprague-Dawley rats (300−350 g) were sacrificed by decapitation, and the brains (whole brain minus cerebellum) were dissected quickly, weighed, and homogenized in 9 volumes per gram of g wet weight of ice-cold 0.32 M sucrose using a rotating pestle on setting 50 (10 up and down strokes). The homogenate was centrifuged at 1000*g* for 10 min at 40 °C. The supernatant was collected and centrifuged at 20000*g* for 20 min at 40 °C. The resulting pellet was resuspended to a protein concentration of 1−8 mg/mL. Aliquots of 5 mL of homogenate were frozen at −80 °C until they were needed for the assay. On the day of the assay, aliquots were thawed at room temperature and diluted with Kreb's 20 mM HEPES buffer, pH 7.0 (at room temperature), containing 4.16 mM $NaHCO_3$, 0.44 mM KH_2PO_4, 127 mM NaCl, 5.36 mM KCl, 1.26 mM $CaCl_2$, and 0.98 mM $MgCl_2$ so that an amount of 25−150 mg of protein is added per test tube. Protein concentration was determined by the Bradford method using bovine serum albumin as the standard. For α7, nonspecific binding was determined in tissues incubated in parallel in the presence of 1 μM MLA and added before the radioligand, and in competition studies, compounds were added in increasing concentrations to the test tubes before addition of approximately 3 nM [^{3}H]MLA (25 Ci/mmol). For α4, nonspecific binding was determined in tissues incubated in parallel in the presence of 1 mM (−)-nicotine, added before the radioligand, and in competition studies, compounds were added in increasing concentrations to the test tubes before addition of approximately 1.0 nM [^{3}H]cytisine. For 5-HT$_3$, nonspecific binding was determined in tissues incubated in parallel in the presence of 1 μM ICS-205930, added before the radioligand, and in competition studies, compounds were added in increasing concentrations to the test tubes before addition of approximately 0.45 nM [^{3}H]GR65630. For all binding assays, 0.4 mL of homogenate was added to test tubes containing buffer, test compound, and radioligand and was incubated in a final volume of 0.5 mL for 1 h at 25 °C. The incubations were terminated by rapid vacuum filtration through Whatman GF/B glass filter paper mounted on a 48-well Brandel cell harvester. Filters were presoaked in 50 mM Tris HCl, pH 7.0, and 0.05% polyethylenimine. The filters were washed two times with 5 mL aliquots of cold 0.9% saline and then counted for radioactivity by liquid scintillation spectrometry. The inhibition constant (K_i) was calculated from the concentration-dependent inhibition of radioligand binding obtained by fitting the data to the Cheng−Prusoff equation.

Patch-Clamp Electrophysiology. Cultured neurons were prepared from Sprague-Dawley rats (postnatal day 3) according to the methods of Brewer (1997). Rats were killed by decapitation, and their brains were removed and placed in ice-cold Hibernate-A medium. Hippocampal regions were gently removed, cut into small pieces, and placed in Hibernate-A medium with 1 mg/mL papain for 60 min at 35 °C. After digestion, the tissues were washed several times in Hibernate-A media and transferred to a 50 mL conical tube containing 6 mL of Hibernate-A medium with 2% B-27 supplement. Neurons were dissociated by gentle trituration and plated onto poly-D-lysine/laminin-coated coverslips at a density of 300−700 cells/mm^2 and transferred to 24-well tissue culture plates containing warmed culture medium composed of Neurobasal-A medium, B-27 supplement (2%), L-glutamine (0.5 mM), 100 U/mL penicillin, 100 mg/mL streptomycin, and 0.25 mg/mL Fungizone. Cells were maintained in a humidified incubator at 37 °C and 6% CO_2 for 1−2 weeks. The medium was changed after 24 h and then approximately every 3 days thereafter. Patch pipets were pulled from borosilicate capillary glass using a Flaming/Brown micropipet puller (P97, Sutter Instrument, Novato, CA) and filled with an internal pipet solution composed of: $CsCH_3SO_3$ (126 mM), CsCl (10 mM), NaCl (4 mM), $MgCl_2$ (1 mM), $CaCl_2$ (0.5 mM), EGTA (5 mM), HEPES (10 mM), ATP−Mg (3 mM), GTP−Na (0.3 mM), phosphocreatin (4 mM), pH 7.2. The resistances of the patch pipets when filled with internal solution ranged between 3 and 6 MΩ.. All experiments were conducted at room temperature. Cultured cells were continuously superfused with an external bath solution containing NaCl (140 mM), KCl (5 mM), $CaCl_2$ (2 mM), $MgCl_2$ (1 mM), HEPES (10 mM), glucose (10 mM), bicuculline (10 μM), CNQX (5 μM), D-AP-5 (5 μM) tetrodotoxin (0.5 μM), pH 7.4. Compounds were dissolved in water or DMSO and diluted into the external bath solution containing a final DMSO concentration of 0.1% and delivered via a multibarrel fast perfusion system (Warner Instrument, Hamden, CT). Whole-cell currents were recorded using an Axopatch 200B amplifier (Molecular Devices, Union City, CA). Analog signals were filtered at $^1/_5$ the sampling frequency, digitized, stored, and measured using pCLAMP software (Molecular Devices). All data are reported as the mean ± SEM. Cell culture reagents were purchased from Invitrogen Corp. (Carlsbad, CA).

hERG Assay. All hERG screening data and concentration response data for PHA-543613 were provided by ChanTest, Inc. (Cleveland, OH). Briefly, HEK293 cells stably expressing hERG were voltage-clamped at −80 mV and step-depolarized to +20 mV for 2 s and then to −40 mV for 2 s once every 10 s. Current amplitude was measured as the peak outward current evoked upon stepping the membrane to −40 mV. Concentration response data for PNU-28987 were generated using CHO-K1 cells stably expressing hERG channels according to published methods.[50] In this case, cells were voltage-clamped at −80 mV and currents were evoked by applying a cardiac action potential (AP) voltage-clamp protocol once per second, and the peak outward current was measured during

the repolarizing phase of the AP wave form. In all cases, test compound was applied after recording a stable baseline, and the evoked current was monitored until a new steady-state amplitude was achieved. Current inhibition was plotted in percent according to

$$\text{inhibition (\%)} = 100 \times \left(1 - \frac{I_{\text{test}}}{I_{\text{control}}}\right)$$

where I_{test} is the current measured in the presence of the test solution and I_{control} is the current measured prior to exposure of the test solution. Each cell served as its own control. The continuous curves were determined according to

$$\text{inhibition (\%)} = 100 \times \left(\frac{[\text{compound}]^n}{[\text{compound}]^n + \text{IC}_{50}{}^n}\right)$$

where [compound] is the concentration of tested compound and the Hill slope n was constrained to unity. All data are presented as the mean ± standard deviation.

Details of the in Vivo Assays. Auditory Gating Assay. Experiments were performed on male Sprague-Dawley rats (Harlan, Indianapolis, IN; weighing 250−300 g) under chloral hydrate anesthesia (400 mg/kg, ip). The femoral artery and vein were cannulated for monitoring arterial blood pressure and administration of drugs or additional doses of anesthetic, respectively. Unilateral hippocampal field potential (EEG) was recorded by a metal monopolar macroelectrode placed into the CA3 region (coordinates: 3.0−3.5 mm posterior from the bregma, 2.6−3.0 mm lateral, and 3.8−4.0 mm ventral; Paxinos and Watson, 1986).[51] Field potentials were amplified, filtered (0.1−100 Hz), displayed, and recorded for on-line and off-line analysis (Spike3). Quantitative EEG analysis was performed by means of fast Fourier transformation (Spike3). The auditory stimulus consisted of a pair of 10 ms, 5 kHz tone bursts with a 0.5 s delay between the first "conditioning" stimulus and second "test" stimulus. Auditory-evoked responses were computed by averaging of responses to 50 pairs of stimuli presented with an interstimulus interval of 10 s. Percentage of gating was determined by the formula

$$\left(1 - \frac{\text{test amplitude}}{\text{conditioning amplitude}} \times 100\right)$$

Amphetamine (*d*-amphetamine sulfate, 1 mg/kg, iv) was administered in order to disrupt sensory gating. Recordings of evoke potentials commenced 5 min after amphetamine administration, and only rats showing gating deficit exceeding 20% were used for subsequent evaluation of α7 nAChR agonists or vehicle. Statistical significance was determined by means of two-tailed paired Student's *t*-test.

Object Recognition Task. Male Sprague-Dawley rats, weighing between 235 and 280 g (at test), were obtained from Charles River Laboratories (Portage, MI; Kingston, NY; or Raleigh, NC) and housed in pairs with free access to food and water on a 12-h light/dark cycle (dark period from 700 to 1900 h). Rats were housed on solid bottom cages with wood chip bedding. All procedures in this study have been approved and conducted in compliance with the Animal Welfare Act Regulations (CFR Parts 1−3) and the "Guide for the Care and Use of Laboratory Animals" (ILAR, 1996), as well as with all internal company policies and guidelines. All testing and object exposures were conducted in a 14 in. × 22 in. × 14 in. semitransparent MaxCart food bin. A clean sheet of cardboard-like Techboard was placed on the floor before each trial. The test arena was indirectly and uniformly illuminated at a low-intensity level of 10−12 Lux. A video camera affixed about 4 feet above the floor of the arena was connected to a monitor and VCR located several feet away from the visually shielded arena. Two types of objects were used in all drug tests reported here: a 500 mL clear Erlenmeyer glass flask and a 500 mL amber-colored bottle (3 in. × 2.25 in. × 8 in.) with a black cap (filled with water). These objects were cleaned after every trial by swabbing with a 70% alcohol solution. Two or more different sets of each object were used to allow air-drying for several minutes between tests.

A 3-day procedure similar to the one used by Moser was utilized as follows.[52] Day 1 involved 2 min of habituation, Techboard floor absorbent side up, and no objects. Day 2 involved 5 min of exploration, Techboard floor absorbent side down, and two identical objects. Objects are placed 2 in. from each of the two sidewalls of the corner. Each animal is allowed as much as 5 min to accumulate a maximum approach time of 20 s to either or both of the identical objects. Consequently, exploratory exposure to the sample object (familiar) was equated between rats by terminating the session after 20 s of object approach. Rats failing to explore the objects for more than 10 s were discarded. In general, greater than 90% of rats achieved this cut off criterion. Day 3 involved 3 min of test duration, Techboard floor absorbent side up, and two dissimilar objects. Approach time to each object was recorded separately and was the major response measure. In these studies, "approach" was defined as the nose of the rat within 2 cm of an object.

Vehicle and compound **14** were administered subcutaneously 30 min before each session. For all experiments, each treatment group consisted of 15 rats at the beginning of the experiments. For each session the animals were placed in the arena with their nose facing away from the objects (when present) and centered on the long side of the arena. Upon placement of the rat in the arena, the experimenter immediately sat in front of the monitor for scoring approach behavior without disturbing the rat. Approach time to each object during the test session was recorded separately and was the major response measure. These data were analyzed using a paired two-tail *t*-test to determine significant differences between novel and familiar approach time, with statistical significance defined by a p value less than 0.05.

Acknowledgment. The authors thank A. Bahinski and K. Erickson for coordinating hERG data collection, the SAM-Chem group for analytical data and chromatography support, the ATG group for in vitro ADME data, and K. Birrell and M. Black for in vivo PK support.

Supporting Information Available: Abbreviations, details for preparation of custom acid fragments, RMA analysis spectra, results from elemental analysis, and results from broad selectivity profiling at Cerep. This material is available free of charge via the Internet at http://pubs.acs.org.

References

(1) (a) Holden, C. Deconstructing Schizophrenia. *Science* **2003**, *299*, 333−335. (b) Sawa, A.; Snyder, S. H. Schizophrenia: Diverse Approaches to a Complex Disease. *Science* **2002**, *296*, 692−695.

(2) Green, M. F.; Braff, D. L. Translating the Basic and Clinical Cognitive Neuroscience of Schizophrenia to Drug Development and Clinical Trials of Antipsychotic Medications. *Biol. Psychiatry* **2001**, *49*, 374−384.

(3) Levin, E. D.; Simon, B. B. Nicotinic Acetylcholine Involvement in Cognitive Function in Animals. *Psychopharmacology* **1998**, *138*, 217−230.

(4) Lead nAChR references: (a) Dani, J. A. Overview of Nicotinic Receptors and Their Roles in the Central Nervous System. *Biol. Psychiatry* **2001**, *49*, 166−174. (b) Picciotto, M. R.; Caldarone, B. J.; King, S. L.; Zachariou, V. Nicotinic Receptors in the Brain; Links between Molecular Biology and Behavior. *Neuropsychopharmacology* **2000**, *22*, 451−465. (c) *Handbook of Experimental Pharmacology: Neuronal Nicotinic Receptors*; Clementi, F., Fornasari, D., Gotti, C., Eds.; Springer: New York, 2000. (d) *Neuronal Nicotinic Receptors: Pharmacology and Therapeutic Opportunities*; Arneric, S. P.; Brioni, J. D., Eds.; Wiley-Liss: New York, 1999.

(5) (a) Freedman, R.; Hall, M.; Adler, L. E.; Leonard, S. Evidence in Post-Mortem Brain Tissue for Decreased Numbers of Hippocampal Nicotinic Receptors in Schizophrenia. *Biol. Psychiatry* **1995**, *38*, 22−33. (b) Marutle, A.; Zhang, X.; Court, J.; Piggott, M.; Johnson, M.; Perry, R.; Perry, E.; Nordberg, A. Laminar Distribution of Nicotinic Receptor Sub-types in Cortical Regions in Schizophrenia. *J. Chem. Neuroanat.* **2000**, *22*, 115−126.

(6) (a) Guan, Z. Z.; Zhang, X.; Blennow, K.; Nordberg, A. Decreased Protein Level of Nicotinic Receptor α7 Subunit in the Frontal Cortex from Schizophrenic Brain. *NeuroReport* **1999**, *10*, 1779−1782. (b) Court, J.; Spurden, D.; Lloyd, S.; McKeith, I.; Ballard, C.; Cairns, N.; Kerwin, R.; Perry, R.; Perry, E. Neuronal Nicotinic Receptors in Dementia with Lewy Bodies and Schizophrenia: α-Bungarotoxin and Nicotine Binding in the Thalamus. *J. Neurochem.* **1999**, *73*, 1590−1597.

(7) Freedman, R.; Coon, H.; Myles-Worsley, M.; Orr-Urtreger, A.; Olincy, A.; Davis, A.; Polymeropoulos, M.; Holik, J.; Hopkins, J.; Hoff, M.; Rosenthal, J.; Waldo, M. C.; Reimherr, F.; Wender, P.; Yaw, J.; Young, D. A.; Breese, C. R.; Adams, C.; Patterson, D.; Adler, L. E.; Kruglyak, L.; Leonard, S.; Byerley, W. Linkage of a Neurophysiological Deficit in Schizophrenia to a Chromosome 15 Locus. *Proc. Natl. Acad. Sci. U.S.A.* **1997**, *94*, 587−592.

(8) Adler, L. E.; Hoffer, L. D.; Wiser, A.; Freedman, R. Normalization of Auditory Physiology by Cigarette Smoking in Schizophrenic Patients. *Am. J. Psychiatry* **1993**, *150*, 1856−1861.

(9) Goff, D. C.; Henderson, D. C.; Amico, E. Cigarette Smoking in Schizophrenia: Relationship to Psychopathology and Medication Side Effects. *Am. J. Psychiatry* **1992**, *149*, 1189−1194.

(10) Ripoll, N.; Bronnec, M.; Bourin, M. Nicotinic Receptors and Schizophrenia. *Curr. Med. Res. Opin.* **2004**, *20*, 1057−74.

(11) (a) Stevens, K. E.; Wear, K. D. Normalizing Effects of Nicotine and a Novel Nicotinic Agonist on Hippocampal Auditory Gating in Two Animal Models. *Pharmacol., Biochem. Behav.* **1997**, *57*, 869−874. (b) Stevens, K. E.; Kem, W. R.; Mahnir, V. M.; Freedman, R. Selective α7-Nicotinic Agonists Normalize Inhibittion of Auditory Response in DBA Mice. *Psychopharmacology* **1998**, *136*, 320−327.

(12) Hajós, M.; Hurst, R. S.; Hoffmann, W. E.; Krause, M.; Wall, T. M.; Higdon, N. R.; Groppi, V. E. The Selective α7 nAChR Agonist PNU-282,987 Enhances GABAergic Synaptic Activity in Brain Slices and Restores Auditory Gating Deficits in Anesthetized Rats. *J. Pharmacol. Exp. Ther.* **2005**, *312*, 1213−1222.

(13) Kitagawa, H.; Takenouchi, T.; Azuma, R.; Wesnes, K. A.; Kramer, W. G.; Clody, D. E.; Burnett, A. L. Safety, pharmacokinetics, and effects on cognitive function of multiple doses of GTS-21 in healthy, male volunteers. *Neuropsychopharmacology* **2003**, *28*, 542−551.

(14) Nagamoto, H. T.; Adler, L. E.; McRae, K. A.; Huettl, P.; Cawthra, E.; Gerhardt, G.; Hea, R.; Griffith, J. Auditory P50 in Schizophrenics on Clozapine: Improved Gating Parallels Clinical Improvement and Changes in Plasma 3-Methoxy-4-hydroxyphenyl-glycol. *Neuropsychobiology* **1999**, *39*, 10−17.

(15) Reviews: (a) Jensen, A. A.; Frolund, B.; Liljefors, T.; Krogsgaard-Larsen, P. Neuronal Nicotinic Acetylcholine Receptors: Structural Revelations, Target Identifications, and Therapeutic Inspirations. *J. Med. Chem.* **2005**, *48*, 4705−4745. (b) Hashimoto, K.; Koike, K.; Shimizu, E.; Iyo, M. α7 nicotinic receptor agonists as potential therapeutic drugs for schizophrenia. *Curr. Med. Chem.* **2005**, *5*, 171−184. (c) Bunnelle, W. H.; Dart, M. J.; Schrimpf, M. R. Design of Ligands for the Nicotinic Acetylcholine Receptors: The Quest for Selectivity. *Curr. Med. Chem.* **2004**, *4*, 299−334. (d) Romanelli, M. N.; Gualtieri, F. Cholinergic Nicotinic Receptors: Competitive Ligands, Allosteric Modulators, and Their Potential Applications. *Med. Res. Rev.* **2003**, *23*, 393−426. (e) Astles, P. C.; Baker, S. R.; Boot, J. R.; Broad, L. M.; Dell, C. P.; Keenan, M. Recent Progress in the Development of Subtype Selective Nicotinic Acetylcholine Receptor Ligands. *Curr. Drug Targets: CNS Neurol. Disord.* **2002**, *1*, 337−348. (f) Schmitt, J. D. Exploring the Nature of Molecular Recognition in Nicotinic Acetylcholine Receptors. *Curr. Med. Chem.* **2000**, *7*, 749−800. Also see references cited within these papers.

(16) (a) Meyer, E. M.; Tay, E. T.; Papke, R. L.; Meyers, C.; Huang, G.-L.; De Fiebre, C. M. 3-[2,4-Dimethoxybenzylidene]anabaseine (DMXB) selectively activates rat alpha 7 receptors and improves memory-related behaviors in a mecamylamine-sensitive manner. *Brain Res.* **1997**, *768*, 49−56. (b) deFiebre, C. M.; Meyer, E. M.; Henry, J. C.; Muraskin, S. I.; Kem, W. R.; Papke, R. L. Characterization of a series of anabaseine-derived compounds reveals that the 3-(4)-dimethylaminocinnamylidine derivative is a selective agonist at neuronal nicotinic alpha7/125I-bungarotoxin receptor subtypes. *Mol. Pharmacol.* **1995**, *47*, 164−171.

(17) Mullen, G.; Napier, J.; Balestra, M.; DeCory, T.; Hale, G.; Macor, J.; Mack, R.; Loch, J.; Wu, E.; Kover, A.; Verhoest, P.; Sampognaro, A.; Phillips, E.; Zhu, Y.; Murray, R.; Griffith, R.; Blosser, J.; Gurley, D.; Machulskis, A.; Zongrone, J.; Rosen, A.; Gordon, J. (−)-Spiro-[1-azabi-cyclo[2.2.2]octane-3,5′-oxazolidin-2′-one], a Conformationally Restricted Analog of Acetylcholine, Is a Highly Selective Full Agonist at the α7 Nicotinic Acetylcholine Receptor. *J. Med. Chem.* **2000**, *43*, 4045−4050.

(18) (a) Macor, J.; Wu, E. Azabicyclic Esters of Carbamic Acids Useful in Therapy. PCT Int. Appl. WO9730998, August 28, 1997. (b) Guendisch, D.; Andrae, M.; Munoz, L.; Tilotta, M. C. Synthesis and evaluation of phenylcarbamate derivatives as ligands for nicotinic acetylcholine receptors. *Bioorg. Med. Chem.* **2004**, *12*, 4953−4962.

(19) Bodnar, A. L.; Cortes-Burgos, L. A.; Cook, K. K.; Dinh, D. M.; Groppi, V. E.; Hajos, M.; Higdon, N. R.; Hoffmann, W. E.; Hurst, R. S.; Myers, J. K.; Rogers, B. N.; Wall, T. M.; Wolfe, M. L. Wong, E. Discovery and SAR of Quiniclidine Benzamides as Agonists of α7 Nicotinic Acetylcholine Receptors. *J. Med. Chem.* **2005**, *48*, 905−908.

(20) Tatsumi, R.; Seio, K.; Fujio, M.; Katayama, J.; Horikawa, T.; Hashimoto, K.; Tanaka, H. (+)-3-[2-(Benzo[*b*]thiophen-2-yl)-2-oxoethyl]-1-azabicyclo[2.2.2]octane as potent agonists for the α7 nicotinic acetylcholine receptor. *Bioorg. Med. Chem. Lett.* **2004**, *14*, 3781−3784.

(21) Biton, B.; Bergis, O. E.; Galli, F.; Nedelec, A.; Lochead, A.; Jegham, S.; Lanneau, C.; Granger, P.; Leonardon, J.; Avenet, P.; Godet, D.; Coste, A.; Vig, X.; Oury-Donat, F.; George, P.; Soubri, P.; Griebel, G.; Scatton B. SSR180711A, A novel selective α7 nicotinic receptor partial agonist. I. Binding profile and in vitro functional characterization. Presented at the 34th Annual Neuroscience Meeting, San Diego, California, October 23−27, 2004; Abstract 583.1.

(22) See Supporting Information for full experimental details.

(23) (a) Wishka, D. G.; Reitz, S. C.; Piotrowski, D. W.; Groppi, V. E., Jr. WO 2002/100857, 2002. (b) Walker, D. P.; Wishka, D. G.; Corbett, J. W.; Rauckhorst, M. R.; Piotrowski, D. W.; Groppi, V. E. WO 2002/100858, 2002. (c) Walker, D. P.; Piotrowski, D. W.; Jacobsen, E. J.; Acker, B. A.; Groppi, V. E. WO 2003/070731, 2003. (d) Rogers, B. N.; Piotrowski, D. W.; Walker, D. P.; Jacobsen, E. J.; Acker, B. A.; Wishka, D. G.; Groppi, V. E. WO 2003/070732, 2003.

(24) The α7 5HT3 chimera assay was previously established as predictive of native α7 nAChR activity; see refs 12 and 19.

(25) Kalgutkar, A. S.; Gardner, I.; Obach, R. S.; Shaffer, C. L.; Callegari, E.; Henne, K.; Mutlib, A.; Dalvie, D.; Lee, J.; Nakai, Y.; O'Donnell, J.; Boer, J.; Harriman, S. A Comprehensive Listing of Bioactivation Pathways of Organic Functional Groups. *Curr. Drug Metab.* **2005**, *6*, 161−225.

(26) Sirota, P.; Mosheva, T.; Shabtay, H.; Giladi, N.; Korczyn, A. D. Use of the Selective Serotonin 3 Receptor Antagonist Ondansetron in the Treatment Of Neuroleptic-induced Tardive Dyskinesia. *Am. J. Psychiatry* **2000**, *157*, 287−289.

(27) (a) Viskin, S. Long QT Syndromes and Torsade de Pointes. *Lancet* **1999**, *354*, 1625−1633. (b) Mitcheson, J. S.; Chen, J.; Lin, M.; Culberson, C.; Sanguinetti, M. C. A Structural Basis for Drug-Induced Long QT Syndrome. *Proc. Natl. Acad. Sci. U.S.A.* **2000**, *97*, 12329−12333.

(28) Compounds screened in Chan Test, hERG Block Comparitor Screen.

(29) Sanguinetti, M. C.; Mitcheson, J. S. Predicting Drug-hERG Channel Interactions That Cause Acquired Long QT Syndrome. *Trends Pharmacol. Sci.* **2005**, *26*, 119−124.

(30) Soglia, J. R.; Harriman, S. P.; Zhao, S.; Barberia, J.; Cole, M. J.; Boyd, J. G.; Contillo, L. G. The Development of a Higher Throughput Reactive Intermediate Screening Assay Incorporating Microbore Liquid Chromatography Microelectrospray Ionization Tandem Mass Spectrometry and Glutathione Ethyl Ester as an in vitro Conjugating Agent. *J. Pharm. Biomed. Anal.* **2004**, *36*, 105−116.

(31) (a) See Supporting Information for LC/MS/MS analysis of NADPH-supplemented human liver microsomal incubations containing **13** and GSH-EE, and for the molecular weight of this conjugate.

(32) Baillie, T. A.; Davis, M. R. Mass spectrometry in the analysis of glutathione conjugates. *Biol. Mass Spectrom.* **1993**, *22*, 319−325.

(33) Dalvie, D. K.; Kalgutkar, A. S.; Khojasteh-Bakht, S. C.; Obach, R. S.; O'Donnell, J. P. Biotransformation reactions of five-membered aromatic heterocyclic rings. *Chem. Res. Toxicol.* **2002**, *15*, 269−299.

(34) Garberg, P.; Ball, M.; Borg, N.; Cecchelli, R.; Fenart, L.; Hurst, R. D.; Lindmark, T.; Mabondzo, A.; Nilsson, J. E.; Raub, T. J.; Stanimirovic, D.; Terasaki, T.; Oeberg, J.-O.; Oesterberg, T. In Vitro Models for the Blood−Brain Barrier. *Toxicol. in Vitro* **2005**, *19*, 299−334.

(35) Seguela, P.; Wadiche, J.; Dineley-Miller, K.; Dani, J. A.; Patrick, J. W. Molecular Cloning, Functional Properties, and Distribution of Rat Brain α7: A Nicotinic Cation Channel Highly Permeable to Calcium. *J. Neurosci.* **1993**, *13*, 596−604.

(36) Compound **14** was screened against a panel of 90 receptors, channels, and enzymes at CEREP and found to have no additional activities.[22]

(37) Krause, M.; Hoffmann, W. E.; Hajos, M. Auditory Sensory Gating in Hippocampus and Reticular Thalamic Neurons in Anaesthetized Rats. *Biol. Psychiatry* **2003**, *53*, 244−253.

(38) (a) Ellenbroek, B. A.; de Bruin, N. M.; van Den Kroonenburg, P. T.; van Luijtelaar, E. L.; Cools, A. The effects of early maternal deprivation on auditory information processing in adult Wistar rats.

Biol. Psychiatry **2004**, *55*, 701−707. (b) O'Neill, H. C.; Rieger, K.; Kem, W. R.; Stevens, K. E. DMXB, an alpha7 nicotinic agonist, normalizes auditory gating in isolation-reared rats. *Psychopharmacology* **2003**, 169, 332−339. (c) Stevens, K. E.; Kem, W. R.; Freedman, R. Selective alpha 7 nicotinic receptor stimulation normalizes chronic cocaine-induced loss of hippocampal sensory inhibition in C3H mice. *Biol. Psychiatry* **1999**, *46*, 1443−1450.

(39) (a) Ennaceur, A.; Delacour, J. A new one-trial test for neurobiological studies of memory in rats. 1: Behavioral data. *Behav. Brain Res.* **1988**, *31*, 47−59. (b) Moser, P. C.; Bergis, O. E.; Jegham, S.; Lochead, A.; Duconseille, E.; Terranova, J.; Caille, D.; Berque-Bestel, I.; Lezoualc'h, F.; Fischmeister, R.; Dumuis, A.; Bockaert, J.; George, P.; Soubrié, P.; Scatton, P. SL65-0155, A Novel 5-HT4 Receptor Partial Agonist with Potent Cognition-Enhancing Properties. *J. Pharmacol. Exp. Ther.* **2002**, *302*, 731−741.

(40) (a) Prickaerts, J.; Sik, A.; van der Staay, F. J.; de Vente, J.; Blokland, A. Dissociable effects of acetylcholinesterase inhibitors and phosphodiesterase type 5 inhibitors on object recognition memory: acquisition versus consolidation. *Psychopharmacology* **2005** *177*, 381−390. (b) Moser, P. C.; Bergis, O. E.; Jegham, S.; Lochead, A.; Duconseille, E.; Terranova, J.; Caille, D.; Berque-Bestel, I.; Lezoualc'h, F.; Fischmeister, R.; Dumuis, A.; Bockaert, J.; George, P.; Soubrié, P.; Scatton, P. SL65-0155, a Novel 5-HT4 Receptor Partial Agonist with Potent Cognition-Enhancing Properties. *J. Pharmacol. Exp. Ther*. **2002**, *302*, 731−741.

(41) Still, W. C.; Kahn, M.; Mitra, A. Rapid Chromatographic Technique for Preparative Separations with Moderate Resolution. *J. Org. Chem.* **1978**, *43*, 2923.

(42) (a) Carpino, L. A. 1-Hydroxy-7-azabenzotriazole. An Efficient Peptide Coupling Additive. *J. Am. Chem. Soc.* **1993,** *115*, 4397−4398. (b) Downing, S. V.; Aguilar, E.; Meyers, A. I. Total Synthesis of Bistratamide D. *J. Org. Chem.* **1999,** *64*, 826−831.

(43) Welstead, W. J., Jr. Enhancing Memory or Correcting Memory Deficiency with Arylamido- and Arylthioamidoazabicycloalkanes. U.S. Patent 4,605,652, August 12, 1986.

(44) Amin, H. B.; Awad, A. A.; Archer, W. J.; Taylor, R. Electrophilic Aromatic Substitution. Part 33. Partial Rate Factors for Protiodetritiation of Benzo[*b*]thiophen; the Resonance-Dependent Reactivity of the Ring Positions. *J. Chem. Soc., Perkin Trans. 2* **1982**, 1489−1492.

(45) Shiotani, S.; Taniguchi, K. Furopyridines. XXI. Synthesis of Cyano Derivatives of Furo-[2,3-*b*]-, -[2,3-*c*]- and -[3,2-*c*]pyridine and Their Conversion to Derivatives Having Another Carbon-Substituent. *J. Heterocycl. Chem.* **1997**, *34*, 493−499.

(46) Soglia, J. R.; Harriman, S. P.; Zhao, S.; Barberia, J.; Cole, M. J.; Boyd, J. G.; Contillo, L. G. The Development of a Higher Throughput Reactive Intermediate Screening Assay Incorporating Micro-bore Liquid Chromatography Micro-electrospray Ionization Tandem Mass Spectrometry and Glutathione Ethyl Ester as an in Vitro Conjugating Agent. *J. Pharm. Biomed. Anal.* **2004**, *36*, 105−116.

(47) Obach, R. S.; Baxter, J. G.; Liston, T. E.; Silber, B. M.; Jones, B. C.; Macintyre, F.; Rance, D. J.; Wastall, P. The Prediction of Human Pharmacokinetic Parameters from Preclinical and in-Vitro Metabolism Data. *J. Pharmacol. Exp. Ther.* **1997**, *283*, 46−58.

(48) Fitch, R. W.; Xiao, Y.; Kellar, K. J.; Daly, J. W. Membrane pOtential Fluorescence: A Rapid and Highly Sensitive Assay for Nicotinic Receptor Channel Function. *Proc. Natl. Acad. Sci. U.S.A.* **2003**, *100*, 4909−4914.

(49) Pabreza, L. A.; Dhawan, S.; Kellar, K. J. [3H]cytisine binding to nicotinic cholinergic receptors in brain. *Mol. Pharmacol*. **1991**, *39*, 9−12.

(50) Hurst, R. S.; Higdon, N. R.; Lawson, J. A.; Clark, M. A.; Rutherford-Root, K. L.; McDonald, W. G.; Haas, J. V.; McGrath, J. P.; Meglasson, M. D. Dopamine receptor agonists differ in their actions on cardiac ion channels. *Eur. J. Pharmacol*. **2003**, *482*, 31−37.

(51) Paxinos, G.; Watson, C. *The Rat Brain in Stereotaxic Coordinates*; Academic Press: Sydney, 1986.

(52) Moser, P. C.; Bergis, O. E.; Jegham, S.; Lochead, A.; Duconseille, E.; Terranova, J.; Caille, D.; Berque-Bestel, I.; Lezoualc'h, F.; Fischmeister, R.; Dumuis, A.; Bockaert, J.; George, P.; Soubrié, P.; Scatton, P. SL65-0155, a Novel 5-HT4 Receptor Partial Agonist with Potent Cognition-Enhancing Properties. *J. Pharmacol. Exp. Ther.* **2002**, *302*, 731−741.

JM0602413